EARTHQUAKE POTENTIAL OF THE CENTRAL VIRGINIA SEISMIC ZONE

Final Technical Report

Research supported by the U.S. Geological Survey (USGS),
Department of the Interior, under USGS grant G13AP00045

Principal Investigator:
Martitia P. Tuttle
M. Tuttle & Associates
128 Tibbetts Lane
Georgetown, ME 04548
Tel: 207-371-2007
E-mail: mptuttle@earthlink.net
URL: http://www.mptuttle.com

Project Period: 8/1/2013-7/31/2015

Program Element III: Research on Earthquake Occurrence, Physics, Effects, Impacts, and Risk
Program Element I: National and Regional Earthquake Hazards Assessments

Key Words: Paleoseismology, Paleoliquefaction, Age Dating

EARTHQUAKE POTENTIAL OF THE CENTRAL VIRGINIA SEISMIC ZONE

Principal Investigator:
Martitia P. Tuttle
M. Tuttle & Associates
P.O. Box 345
Georgetown, ME 04548
Tel: 207-371-2007
E-mail: mptuttle@earthlink.net

ABSTRACT

During reconnaissance along 119 km of six rivers in the meisoseismal area of the 2011 moment magnitude, **M**, 5.8 Virginia, earthquake, we verified the presence of paleoliquefaction features along the South Anna River and Stigger Creek, a tributary to the Rivanna River, and found additional liquefaction features along the James, Mattaponi, and Pamunkey Rivers. On the basis of weathering characteristics of the liquefaction features as well as radiocarbon and OSL dating of sediments in which liquefaction features occur, at least two episodes of earthquake-induced liquefaction are inferred. A few small (≤ 3 cm) sand dikes and strata-bound soft-sediment deformation structures at three sites on the James and Pamunkey Rivers probably formed during a recent earthquake in the past 500 years. The three sites occur in the southeastern part of the study area suggesting that the earthquake may have been located in this area or farther to the southeast. Large uncertainties about this event will remain until additional data can be brought to bear on its interpretation. Bioturbated and weathered sand dikes (≤ 7 cm) and sills at sites on the Mattaponi, Pamunkey, and South Anna Rivers, as well as Stigger Creek, are likely to be prehistoric in age and are currently assumed to have formed during a single Late Holocene earthquake in the past 4,500 years. The size and areal distribution of the liquefaction features suggest that the Late Holocene event was of **M** ≥ 6 and located farther to the east than the 2011 Virginia, earthquake. Additional study is needed to map the full extent and to constrain the ages of liquefaction features in order to better assess the earthquake potential of the Central Virginia seismic zone.

INTRODUCTION

On August 23, 2011, a moment magnitude, **M**, 5.8 earthquake occurred near Mineral, Virginia, about 50 km east of Charlottesville, 60 km northwest of Richmond, and 130 km southwest of Washington, D.C. (Figure 1). The earthquake was widely felt along most of the eastern seaboard from Georgia to Canada and strongly felt in central Virginia (Figure 2). It caused damage to residences and schools in the epicentral area as well as to building, bridges, and monuments in Washington, D.C. and southern Maryland and Delaware (Martin et al., 2011). Minor damage was reported as far away as New Jersey, New York, and South Carolina. Peak ground acceleration (PGA) of 0.27 g, measured 18 km from the epicenter at the North Anna nuclear power plant, was greater than the ground motion expected to be exceeded in a 50-year period with a probability of 2% (Petersen et al., 2008). The 2011 mainshock and some of the aftershocks were characterized by high stress drops in the 50-100 MPa range, comparable to those of the 1988 **M** 5.9 Saguenay, Canada, 2010 **M** 7.1 Darfield, New Zealand, and 2011 **M** 6.3 Christchurch, New Zealand, earthquakes (Ellsworth et al., 2011).

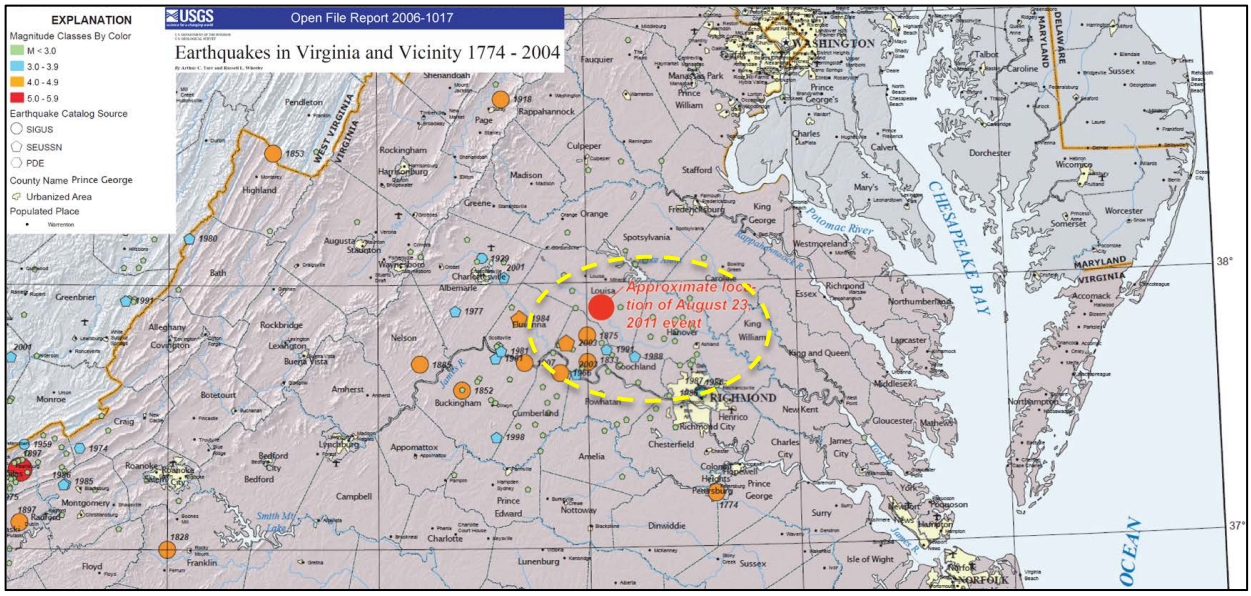

*Figure 1. Earthquakes in Virginia, and vicinity from 1774-2004 (Tarr and Wheeler, 2006), showing concentration of seismicity (see explanation on map) in the Central Virginia seismic zone, location of the 2011 **M** 5.8 earthquake (red circle) within the zone, and area within which paleoliquefaction features have been found during this and previous studies (yellow dashed ellipse).*

The 2011 **M** 5.8 earthquake occurred in the central Virginia seismic zone (CVSZ), a source of persistent, low-level earthquake activity that extends 120 km from about Culpepper to Amelia and 145 km from about Richmond to Lynchburg, Virginia (Figure 1; Bollinger and Sibol, 1985). Seismicity in the CVSZ ranges in depth from about 3 to 13 km (Wheeler and Johnston, 1992). The geology in the region is very complex (Spears et al., 2004). Seismicity has been difficult to attribute to any known geologic structure and may occur both above and below the Appalachian detachment (Tuttle and Hartleb, 2012). The 2011 **M** 5.8 earthquake is thought to be the result of reverse slip on a northeast-trending, southeast-dipping fault in the Eastern Piedmont thrust sheet and within a belt of Triassic basins associated with rifting and opening of the Atlantic Ocean (Ellsworth et al., 2011). The fault responsible for the **M** 5.8 earthquake has been difficult to ascertain because it apparently did not rupture the surface. The mainshock and more than thirty aftershocks ranging up to **M** 4.5 occurred within the Chopawamsic formation, between the Chopawamsic fault to the northwest and the Spotsylvania fault zone to the southeast (Spears, 2012). The structure defined by aftershock hypocenters has been named the Quail fault (Horton et al., 2012) though slip on a previously unrecognized Paleozoic or Mesozoic fault is a possibility (Chapman, 2013).

The 2011 **M** 5.8 earthquake is the largest mainshock to have occurred in the CVSZ during the historical period and has raised concerns about the earthquake potential of the seismic zone located only 130 km from the nation's capital (Figure 1). Like the 1988 **M** 5.9 Saguenay, Quebec, and the 2011 **M** 6.3 Christchurch, New Zealand, events, the 2011 **M** 5.8 Virginia, earthquake was not associated with surface rupture but did induce liquefaction. Compared to the Saguenay and Christchurch events, the Virginia earthquake apparently produced only a few small sand blows in a relatively small area (5 km^2) (Tuttle et al., 1990; Cubrinovski et al., 2011; Martin et al., 2011). This may be due, in part, to the smaller magnitude of the Virginia event, but

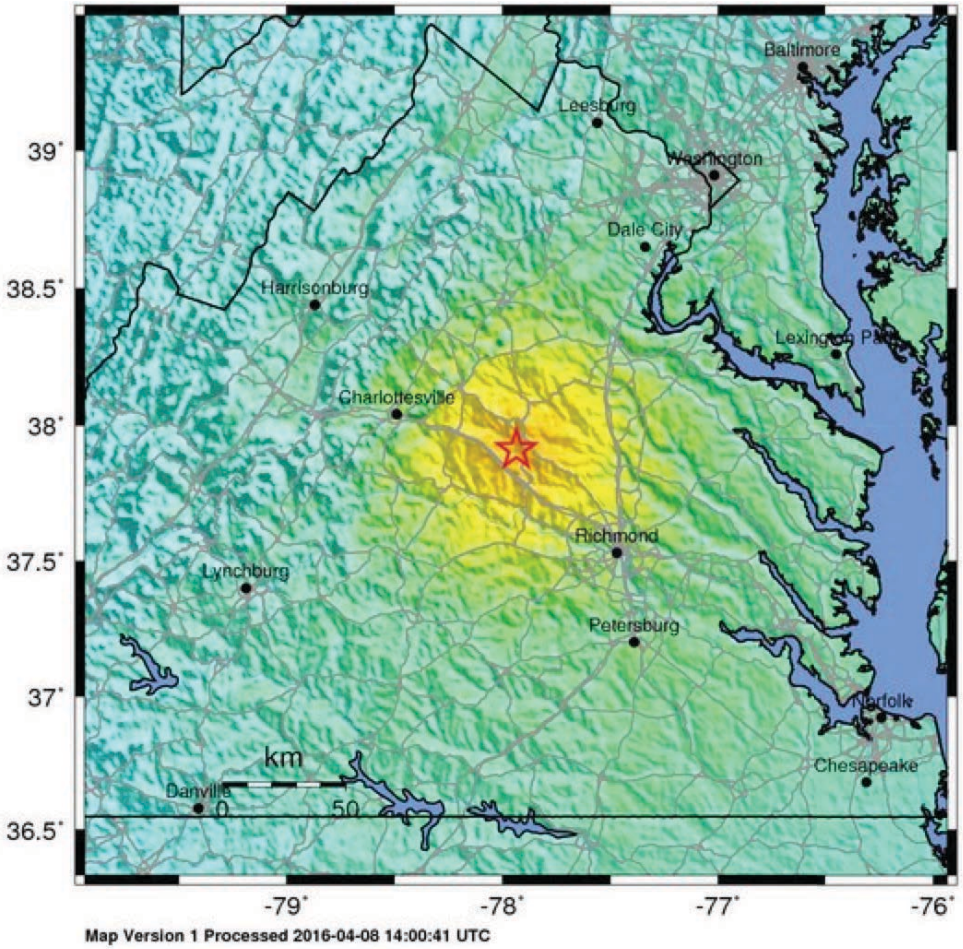

PERCEIVED SHAKING	Not felt	Weak	Light	Moderate	Strong	Very strong	Severe	Violent	Extreme
POTENTIAL DAMAGE	none	none	none	Very light	Light	Moderate	Mod./Heavy	Heavy	Very Heavy
PEAK ACC.(%g)	<0.007	0.08	1.0	5.0	8.8	15	27	47	>83
PEAK VEL.(cm/s)	*<0.003*	*0.04*	*0.5*	*3.0*	*6.5*	*14*	*30*	*63*	*>136*
INSTRUMENTAL INTENSITY	I	II-III	IV	V	VI	VII	VIII	IX	X+

Scale based upon Atkinson & Kaka, 2007

Figure 2. USGS shakemap of the August 23, 2011 Virginia, earthquake (http://earthquake.usgs.gov/earthquakes/eventpage/se609212#shakemap). Instrumental intensities of VI occurred over a large portion of central Virginia.

also to the limited distribution of liquefiable sediments in the epicentral area (Tuttle and Busch, 2011).

This paleoliquefaction study takes advantage of the rare opportunity provided by the 2011 **M** 5.8 Virginia, earthquake to study liquefaction induced by a moderate earthquake in the eastern U.S. and to compare the size and areal distribution of paleoliquefaction features in the CVSZ with those that formed during the 2011 earthquake. Insights gained during this study, in combination with previously collected paleoliquefaction data, will help to advance the understanding of the earthquake potential of the CVSZ.

This research was conducted in cooperation with Mark Carter of the U.S. Geological Survey, who participated in fieldwork and whose knowledge of local geology was especially valuable. Jake Dunahue assisted with river reconnaissance and report writing, Cameron Karrenbauer tabulated data, and Kathy Tucker updated the regional map of liquefaction sites. Beta Analytic, Inc. performed radiocarbon dating and Steve Forman of the Geoluminescence Dating Research Laboratory conducted optically stimulated luminescence (OSL) dating for this project. Geotechnical data previously collected at bridge crossings was provided by Carl Benson and Mike Hall of the Virginia Department of Transportation. Preliminary results of this research have been presented at several meetings (Tuttle, 2015; Tuttle et al., 2015; Carter et al., 2016).

PREVIOUS LIQUEFACTION STUDIES IN THE CENTRAL VIRGINIA SEISMIC ZONE

During a paleoliquefaction study conducted in the mid-1990s, cutbank exposures of rivers in the region were searched for paleoliquefaction features. Several weathered sand dikes (1 to 10 cm wide) were found at three sites in the CVSZ (Obermeier and McNulty, 1998; Dominion, 2004). The paleoliquefaction sites occur on the James, Rivanna, and South Anna Rivers. These sites range from 18 to 30 km from the epicenter of the 2011 **M** 5.8 Virginia, earthquake (Figure 3; gray squares). Along some of the rivers that were searched, liquefiable sediment was rare or absent. Where liquefiable sediment was present, it ranged from 1,000-3,000 years in age (Dominion, 2004), limiting the length of the paleoseismic record. The paleoliquefaction features were attributed to at least one, and possibly three, moderate earthquakes during the Holocene. The apparent lack of widespread liquefaction features was interpreted as evidence that an earthquake of **M** > 7 had not occurred in the CVSZ during the past 10,000 years, though an earthquake in the **M** 6 to 7 range was not ruled out (Obermeier and McNulty, 1998; Dominion, 2004).

During a post-earthquake survey in the epicentral area of the August 23, 2011, **M** 5.8, Virginia, earthquake, four small sand blows were found in or near the South Anna River near Yancy Mill and about 5 km upstream near the Bend of River Road, indicating that the moderate earthquake induced liquefaction at these locations (Martin et al., 2011). These liquefaction features are thought to occur up dip from the fault rupture. The sand blows were composed of coarse sand. In two cases, the slurry of water and sediment appeared to have vented through animal holes or burrows. The sediments in the epicentral area are predominately clayey residuum developed in igneous and metamorphic rock (Figure 3; Soller and Reheis, 2004). Therefore, it is not surprising that liquefaction was not more severe or pervasive during this earthquake (Martin et al., 2011). On August 25th, Frank Syms and Randy Cumbest of Fugro consultants performed aerial reconnaissance of the epicentral region, including portions of the James River to the southeast (Green et al., 2015). They found no evidence of liquefaction or lateral spreading, which is not surprising given the small size of the sand blows in the epicentral area and the heavy forest and vegetative cover across much of the region.

It should be noted, that the initial survey for liquefaction features was limited to a few floodplains and bridge crossings of the South Anna River in the epicentral area. Four days after the earthquake, Hurricane Irene struck Virginia, and was followed about a week later by heavy rain from remnants of tropical storm Lee. High river levels resulting from precipitation during these storms washed away sand blows that formed in and adjacent to the South Anna River, and possibly in other locations as well.

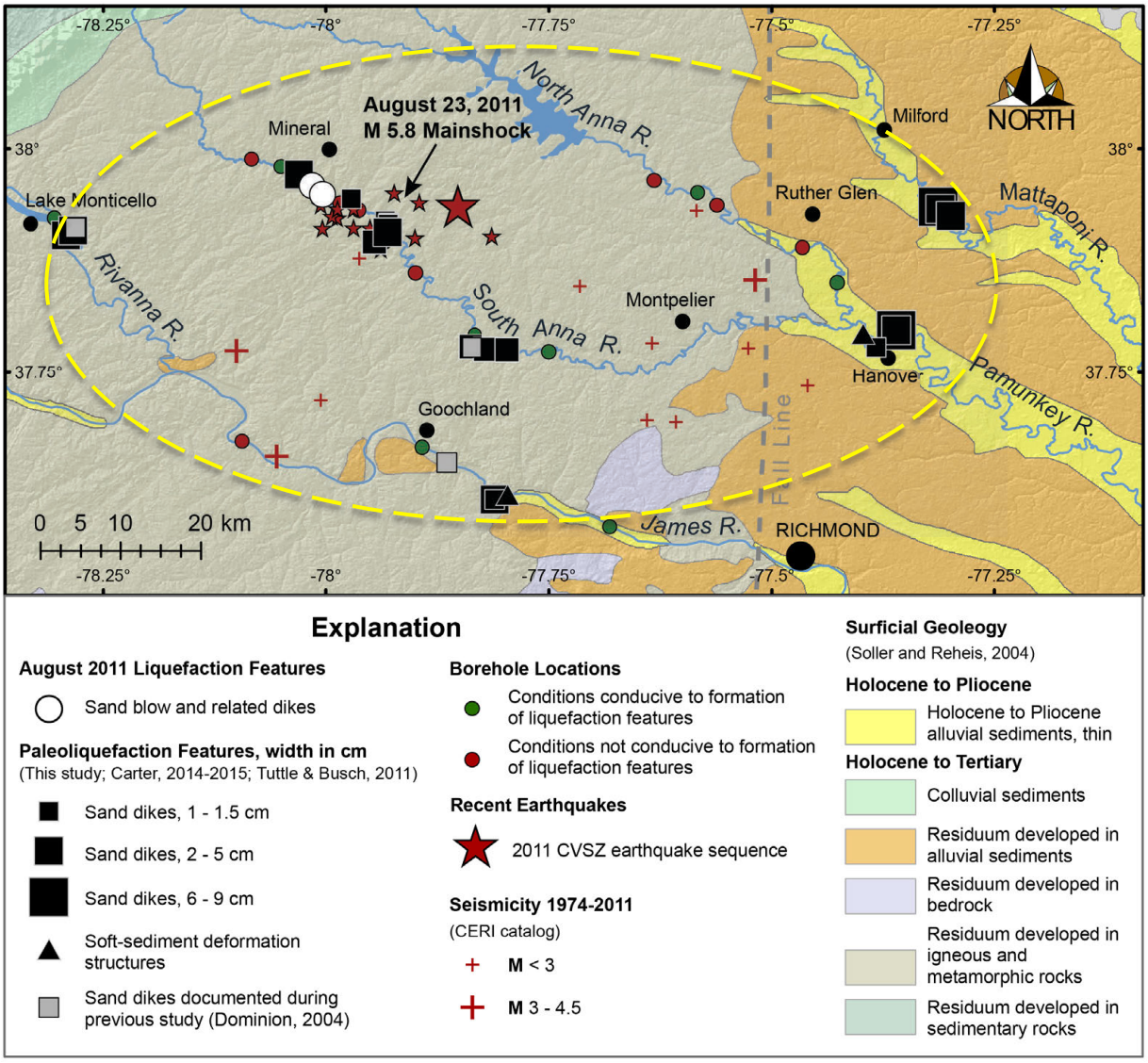

Figure 3. Geologic map of the study region showing locations of the 2011 Virginia, earthquake sequence, small sand blows that formed in the epicentral area during that event, and paleoliquefaction features found during this and other studies.

During post-earthquake river reconnaissance performed three months after the mainshock, no modern liquefaction features were found on floodplains or in cutbank exposuress of the South Anna River in the Yancy Mill area or downstream from there for a distance of 24 kilometers (Tuttle and Busch, 2011). However, possible paleoliquefaction features were found at eight sites along the South Anna River (Figure 3, black squares). One of these sites occurs in the vicinity of a possible liquefaction feature found during the mid-1990s paleoliquefaction study (Obermeier and McNulty, 1998; Dominion, 2004). The features identified in 2011 as most likely to be the result of earthquake-induced liquefaction are dike-like structures that have lateral continuity, branch upward, and are filled with sandy sediment containing clasts of the host deposit. At a couple of the South Anna River sites, animal burrows and root casts appeared to have been utilized as near-surface pathways for liquefied and fluidized sediment. Also, the features were somewhat bioturbated and weathered indicating that they are prehistoric, probably Holocene, in

age. In general, the dike-like features appeared to increase in width, from 1-1.5 cm to 2-5 cm, towards the east. Given that no recent liquefaction features were found along the South Anna River and that the paleoliquefaction features appeared to be getting larger in size towards the east, it was suggested that the prehistoric earthquake(s) responsible for the paleoliquefaction features may have been larger, and/or located farther to the east, than the 2011 **M** 5.8 event (Tuttle and Busch, 2011). Subsequently, similar paleoliquefaction features were found at the Horseshoe site upriver from Yancy Mill, underscoring that additional reconnaissance for paleoliquefaction features was warranted (Carter, 2015).

RECONNAISSANCE FOR EARTHQUAKE-INDUCED LIQUEFACTION FEATURES

Systematic surveys of cutbank exposures were conducted along selected portions of the James, Mattaponi, North Anna, Pamunkey, Rivanna (and tributary Stigger Creek), and South Anna Rivers. The South Anna River was resurveyed along the portion of the river where likely paleoliquefaction features were found within 5 km of the epicenter of the 2011 earthquake (Figure 3). Portions of the North Anna, Pamunkey, and Mattaponi Rivers were surveyed east of the Fall Line. The James and Rivanna Rivers were surveyed in the vicinity of liquefaction sites found during a previous paleoliquefaction study (Obermeier and McNulty, 1998; Dominion, 2004). Geotechnical data provided by the Virginia Department of Transportation indicate that sandy sediment susceptible to liquefaction are present along the selected portions of the James, Pamunkey, and Rivanna Rivers (Figure 3, green circles).

James River

Setting

River cutbanks along two segments of the James River west of Richmond were searched for earthquake-induced liquefaction features (Figure 3). These river segments include 13 km between the Rt. 522 bridge at Goochland and the mouth of Genito Creek and 8 km between the Rt. 45 bridge at Cartersville and West View. Along these segments, the river is flanked by fluvial terraces, although bedrock outcrops in a few places. At the time of reconnaissance, overall exposure was only fair and limited to several slump scarps and the lower portion of the banks that were eroded by wave action. Cutbanks in the fluvial terraces ranged from 1.5 to 5.0 m in height. Most exposures were of the lower 0.5 to 1.0 m of the banks; whereas, the upper 3.5-4 m was usually covered by tree roots, grass, and shrubs.

During the survey along the Goochland-Genito Creek segment of the river, the James River was very low. The river banks were heavily vegetated near Rt. 522 and for about 2 km downstream at which point exposure improved. Cutbanks measured 2 to 5 m in height and revealed interbedded silt and sand, with occasional layers of thick reddish, brown silt. About 7 km downstream from the Rt. 522 bridge, the river shallowed and bedrock was exposed in the stream bed and along the banks. The best exposures occurred in a relatively sharp bend downstream from this bedrock high. In the river bend, 4 m-high cutbanks revealed mottled silt overlying interbedded silt, clayey silt, and silty sand.

During the survey along the Cartersville-West View segment of the river, the James had risen about 0.6 m in response to 3 cm of precipitation the previous night. The increase in river level reduced exposure of the lower portion of the banks. Nevertheless, there were several 2.5 to 4 m-high exposures provided by slump scarps, which revealed mottled silt and interbedded silt and

sand. In the vicinity of the Rt. 45 bridge at Cartersville, cutbanks were 2.5 m high and exposed mottled, reddish and tan, silt. Probing below the base of the cutbank suggested similar materials to 0.7 m depth and interbedded silt and sand from 0.7-1.5 m depth. From about 4 km downstream from Cartersville to West View, bedrock outcrops along the southern bank of the river; whereas, a 0.5 to 1.0 km wide fluvial terrace occurs along the northern flank of the river (Marr, 2002).

During reconnaissance, sediment and soft-sediment deformation structures, including those interpreted as earthquake-induced liquefaction features, were recorded at three sites along the James River (Figure 3). Sites JR1 and JR2 are located along the Goochland-Genito Creek portion of the river and JR10 is located along the Cartersville-West View section. These sites and their sedimentary characteristics and the deformation structures are described below.

Observations

Site JR1 is located on the south side of the river about 10.4 km downstream from the Rt. 522 bridge at Goochland and about 1 km northeast of Fine Creek Mills (Figure 3). The cutbank at JR1 measured 4 m above water level (awl) at the time of the survey. The upper 2.5 m was mostly vegetated but the lower 1.5 m was well exposed. The cutbank revealed the following sedimentary section: mottled, brownish red and gray, clayey silt, 5 cm-thick silty, very fine sand 15-cm-thick mottled silt, mottled clayey silt of similar thickness, 5 cm-thick silty, very fine sand, interbedded silt and silty, very fine sand of similar thickness, and 15 cm-thick gray silt (Figure 4). Beneath the silt was a thin organic layer of twigs and leaves. Four sand dikes were identified in the exposed section. All four dikes originated in the lower 5-cm-thick layer of silty, very fine sand. The most prominent sand dike crosscut the overlying clayey silt and silt layers and terminated 58 cm above the water level within the uppermost silty, very fine sand (Figure 4). The most prominent dike was up to 2.5 cm wide and had a strike and dip of N28°E, 80°NW. The three other sand dikes, with widths of 3 cm, 1.5 cm, and 0.6 cm, pinched out at various heights within the clayey silt.

A sample of charcoal (JR1-C1) was collected from the silty, sand layer in which the prominent dike terminates. The sample yielded a 2-sigma calibrated radiocarbon age of 305-270, 215-150, and 15-post 0 (or calibrated calendar date of A.D. 1645-1680, A.D. 1735-1800, A.D. 1935-Post 1950) (Table 1) and provides a maximum constraining age for the sand dike. A sediment sample (JR1-1) was also collected from the same layer and yielded an OSL age of 230 ± 20 yr (or date of A.D. 1760-1800) (Table 2). These results are remarkably similar. A leaf sample (JR1-C2) was collected 22 cm below the source bed of the dikes from the organic layer. The sample yielded a radiocarbon age of 280-170, 150-Post 0 (or A.D. 1670-1780, A.D. 1800-Post 1950) very similar to the age for JR1-C1. Radiocarbon dating of organics within the exposed sediment suggests that it was deposited and the sand dikes formed since 280 yr B.P. (or A.D. 1670). OSL dating of the layer in which the prominent dike terminates suggests that the dikes may have formed after A.D. 1760.

Site JR2 is about 1.5 km downstream from JR1 and along the same side of the river (Figure 3). The cutbank height and overall sedimentary section is similar to that at JR1. The lower 1 m of the cutbank was exposed, while the upper 3 m of the bank was covered with vegetation. The exposed section consisted of mottled silt underlain by silty, very fine sand, clayey silt, and interbedded sand and silt, followed by gray silt and an organic layer near the base of the cutbank.

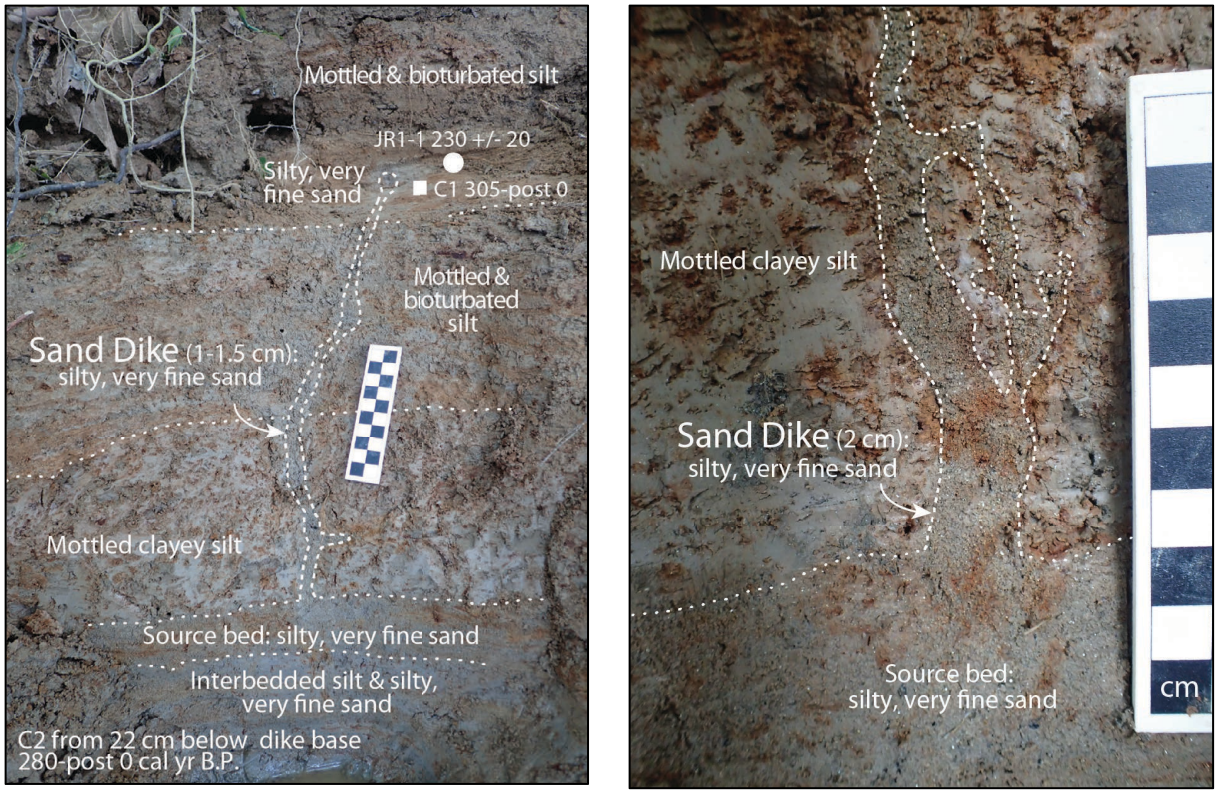

Figure 4. Photographs of sand dikes at site JR1, on scale, black and white intervals represent centimeters: (Left) Sand dike originates in a silty, fine to very fine sand and extends upsection crosscutting overlying clayey silt and silt layers and terminates within the uppermost silty sand layer; white square indicates location of C14 sample and white circle indicates location of OSL sample; C14 result shown as range of calibrated radiocarbon ages in years B.P. (or before A.D. 1950) and OSL result shown as OSL age relative to A.D. 2010; (Right) Close-up of the base of sand dike and the source layer from which it originates.

Soft-sediment deformation structures, including pseudo-nodules and load casts, occurred within interbedded sand and silt above the gray silt (Figure 5). The layer in which the deformation structures formed is very similar to the silty sand layer at JR1 in which sand dikes originate. A sample of leaves (JR2-W1) was collected at 15 cm above the water level from the organic layer below the gray silt. The sample yielded a 2-sigma calibrated radiocarbon age of 305-265, 215-145, and 20-post 0 (or date of A.D. 1645-1685, A.D. 1735-1805, A.D. 1930-Post 1950), very similar to dates of samples from site JR1, supporting an historic age for the sediment and liquefaction features.

Site JR3 is located along the north bank of the river and about 4 km downstream from the Rt. 45 bridge at Cartersville. At the site, the bank measured about 4.25 m awl. Although the upper 0.5 m of the bank was vegetated, a slump scarp provided good exposure of the lower 3.75 m. The cutbank revealed the following sequence of sediment: 1 m of reddish silt underlain by 3.25 m of interbedded reddish silt and cross-bedded sand containing magnetite. Probing suggested that interbedded sand and silt continued to 60 cm below the base of the cutbank where an indurated layer, probably ferricrete, was encountered. In the upper half of the section, the contacts between thick silt beds and thin sand beds are bioturbated. In the lower half of the section, a

Table 1. Radiocarbon dating of organic samples in the CVSZ.

River Site#-Sample# Lab #	$^{13}C/^{12}C$ Ratio	Conventional Radiocarbon Age Yr B.P.[1]	Calibrated Radiocarbon Age Yr B.P.[2]	Calibrated Calendar Date A.D./B.C.[2]	Sample Description
James					
JR1-C1 Beta-414595	-25.8	220 ± 30	305-270 215-150 15-Post 0	AD 1645-1680 AD 1735-1800 AD 1935- Post 1950	Charred material; from sand layer in which largest dike terminates
JR1-C2 Beta-414596	-28.6	130 ± 30	280-170 150- Post 0	AD 1670-1780 AD 1800-Post 1950	Plant material; from leaf mat 22 cm below dike base
JR2-W1 Beta-414597	-28.7	210 ± 30	305-265 215-145 20-Post 0	AD 1645-1685 AD 1735-1805 AD 1930-Post 1950	Plant material; from decomposing leaf mat 15 cm above water level (awl)
No. Anna R.					
NA3-W1 Beta-414589	-30.3	180 ± 30	295-255 225-135 115-110 95-85 30-Post 0	AD 1655-1695 AD 1725-1815 AD 1835-1840 AD 1855-1865 AD 1920-Post 1950	Plant material; from leaf mat 20 cm awl
Pamunky					
PR3-W1 Beta-414590	-27.0	104.5 ± 0.3 pMC	Post 0	Post 1950	Plant material; collected 3 cm awl
PR5-C1 Beta-414591	-26.0	4800 ± 30	5595-5575 5550-5475	BC 3645-3625 BC 3600-3525	Charred material; from mottled silt 25 cm awl
PR6-W1 Beta-414592	-29.7	270 ± 30	430-375 320-285 165-155	AD 1520-1575 AD 1630-1665 AD 1785-1795	Plant material; from leaf layer at water level
Rivanna					
RR1-W1 Beta-414594	-29.7	220 ± 30	305-270 215-150 15-Post 0	AD 1645-1680 AD 1735-1800 AD 1935-Post 1950	Plant material; from organic layer within interbedded silt and sand 22 cm awl
So. Anna					
SoAR100-C1 Beta-414599	-26.3	3930 ± 30	4435-4290	BC 2485-2340	Plant material; from sandy unit 125 cm below water level

[1] Conventional radiocarbon ages in years B.P. or before present (1950) determined by Beta Analytic, Inc. Errors represent 1 standard deviation statistics or 68% probability.

[2] Calibrated age ranges as determined by Beta Analytic, Inc., using the Pretoria procedure (Talma and Vogel, 1993; Vogel et al., 1993). Ranges represent 2 standard deviation statistics or 95% probability.

Table 2. Optically stimulated luminescence ages on quartz grains from sediment in the CVSZ.

Sample Number	Lab Number	Cosmic Dose Rate (mGray/yr)[1]	Dose Rate (mGray/yr)	OSL Age (Yr)[2]	Sample Description
JR1-1	BG4000	0.14 ± 0.01	2.34 ± 0.12	230 ± 20	From layer in which dike terminates
SOAR7-1	BG4001	0.18 ± 0.01	1.84 ± 0.09	8720 ± 500	From host sediment crosscut by dikes
SC1-1	BG4002	0.16 ± 0.01	3.57 ± 0.18	9020 ± 500	From layer in which dikes originate

[1] Cosmic dose rate calculated from parameters in Prescott and Hutton (1994).
[2] Systematic and random errors calculated in a quadrature at one standard deviation. Datum year is AD 2010.

thick sand layer appeared to be deformed (Figure 6). Upon closer examination, an open root mold, tubular structures, and flecks of organics could be seen within the deformed sands. The deformation was clearly due to bioturbation.

Interpretations

The sand dikes at JR1 are likely to be an earthquake-induced liquefaction features. They originate within silty, very fine sand and intrude and crosscut overlying sediment. At JR2, only 1.5 km downstream from JR1, load casts and pseudo-nodules occur in a sandy layer similar to and likely correlative with the source bed of the sand dikes at JR1. Although they can form as the result of syn-depositional processes, strata-bound soft-sediment deformation structures can form also as the result of earthquake-induced liquefaction (Sims, 1973 and 2012; Tuttle and Atkinson, 2010). Given their proximity to the sand dikes at JR1 and the likely correlation of the sandy layer at the two sites, the soft-sediment deformation features at JR2 are likely to be earthquake-induced liquefaction features and to have formed at the same time as the dikes at JR1. Dating at JR1 and JR2 suggests that the sediment along this bank of the river was deposited and that the liquefaction features formed since 305 yr B.P. (or A.D. 1645).

Given that it is the largest known historical earthquake to have occurred in the CVSZ, the 2011 **M** 5.8 earthquake would seem the most likely cause of the liquefaction features. According to the magnitude-distance relation of Castilla and Audemard (2007), a **M** 5.8 earthquake could induce liquefaction and the formation of sand blows up to 38 km from its epicenter. The James River liquefaction sites are about 35 km from the epicenter. Also, Sims (1973) found that strata-bound liquefaction features can form at lower shaking intensities of VI. As shown on the shakemap of the August 23, 2011 earthquake, instrumental intensities of VI occurred west of Richmond in the vicinity of JR2 (Figure 2). However, river levels in the region were very low at the time of the 2011 Virginia earthquake. According to USGS surface-water daily statistics (http://waterdata.usgs.gov/nwis/dvstat?referred_module=sw) for monitoring stations on the James River, river discharge was so low on August 23, 2011 that the source beds at JR1 and JR2 would not have been saturated, and therefore, could not have liquefied. Additional information about liquefaction induced by this recent event, as well as review of historical earthquakes in the region, will be needed to unravel this mystery.

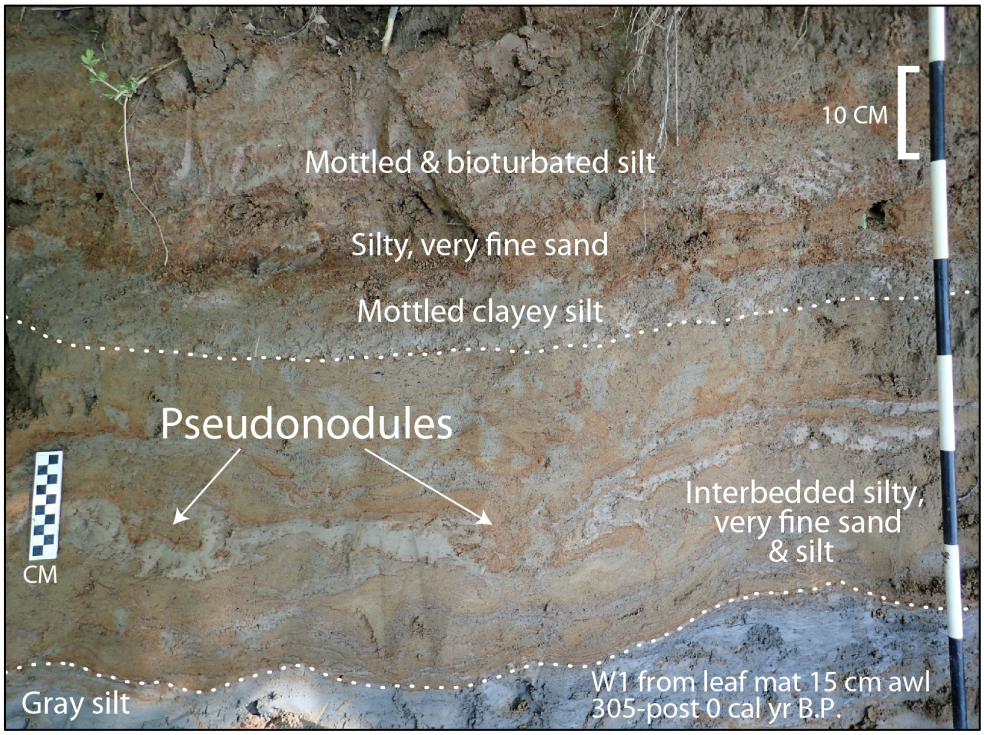

Figure 5. Photographs of soft-sediment deformation structures at site JR2: Pseudo-nodules occur within interbedded sand and silt at the site. C14 result of sample collected from organic layer below gray silt is shown as range of calibrated radiocarbon ages in years B.P. (or before A.D. 1950). On small scale, black and white intervals represent centimeters; on large scale, black and white intervals represent decimeters.

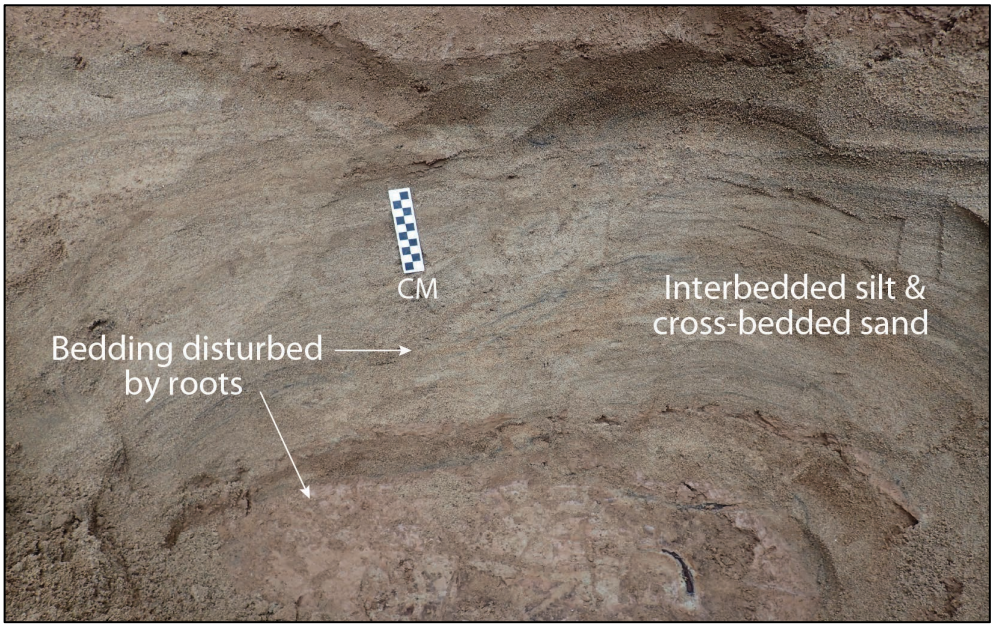

Figure 6. Interbedded, reddish silt and cross-bedded sand containing magnetite. Bedding adjacent to scale is disturbed by bioturbation. Partial roots and root casts filled with sediment can be seen in the floor of the pit (bottom). Black and white intervals on small scale represent centimeters.

Mattaponi River

Setting

East of Ruther Glen, we searched for earthquake-induced liquefaction features along a 23 km segment of the Mattaponi River downriver from the Rt. 654 bridge (Figure 3). Quaternary fluvial deposits of interbedded silt and sand overlying pebbly and cobbly sand have been mapped along this segment of the river (Virginia Division of Mineral Resources, Geologic Map of Virginia, 1993). Terraces are inset into a lower Tertiary unit, known as the Aquia formation, composed of glauconitic quartz sand high in the section and thick, variably shelly, clay-silt, lower in the section. Another Tertiary unit, the Eastover formation, also occurs along this section of the river. The Eastover is sparsely diatomaceous, variably shelly, and composed of sand, silt, and clay. The 23 km segment of the river are subdivided into three portions and described below.

Along the upper 3-km-long portion of the river, cutbanks ranged from 1-5 m in height and exposed unconsolidated Quaternary or indurated Tertiary deposits. Occasionally, Tertiary and Quaternary deposits could be seen in the same section. Near the Rt. 654 bridge, clayey silt was underlain by interbedded sand and clay below water level. Downstream, silty fine sand was underlain by fine sand that coarsens with depth to pebbly sand. Elsewhere, the same sequence was underlain by indurated silt and very fine sand interpreted to be part of the Aquia. Conditions for earthquake-induced liquefaction improved near Campbell's Millpond creek where interbedded silt and sand was underlain by very fine to fine sand. This sequence was exposed along 1.75-m-high cutbanks in a large meander bend. Sites MR1 and MR2 are located along this meander bend. Exposure was nearly continuous along much of this portion of the river. However, the last 1 km alternated between vegetated banks and 4-5 m-high cutbanks exposing the Aquia.

Along the middle 6-km-long portion of the river, the banks were mostly vegetated but there were occasional cutbanks that ranged from 1-2 m in height and exposed primarily the Aquia formation. At about 6.5 km downstream from the Rt. 654 bridge, a 1.5-2 m cutbank revealed mottled silty fine sand to silt. Use of a soil probe suggested sand and pebbly sand extended to 0.7 m below the base of the cutbank. Towards the end of this portion of river, cutbanks exposed reddish, very fine sandy, silt and pebbly sand. Conditions were not especially suitable for the formation of earthquake-induced liquefaction and no liquefaction features were found along this portion of the river.

Along the lower 14-km-long portion of the river, cutbanks were 1-2 m in height and exposed mottled silty, very fine sand and silt. Probing below the base of the cutbank to 1.5 m depth, we found interbedded silt and sand with an occasional layer of pebbly sand. Site MR3 is located about 9.5 km downriver from the Rt. 654 bridge where a 2-m-high cutbank revealed mottled, very fine sandy, silt. From 9.5-14.0 km downriver from the bridge, cutbanks were mostly vegetated; however, there were a few cutbank exposures in river bends. The exposures were 1.5-2 m in height and revealed mottled silt underlain by silty, very fine sand. Use of the soil probe suggested the presence of silty, very fine sand, fine to medium sand, and pebbly sand to a depth of 1.5 m below the water table. Along this portion of the river, conditions appear to be favorable for the formation of earthquake-induced liquefaction features; however, exposure was quite limited.

Three sites, MR1, MR2, and MR3, were documented along the 23 km segment of the Mattaponi River (Figure 3). Sediment and soft-sediment deformation structures, including those interpreted as earthquake-induced liquefaction features, at the three sites are described below.

Observations

Site MR1 is located 1.8 km downstream from the Rt. 654 bridge. The site is along the north side of the river where there was a 0.95 m-high cutbank in Holocene alluvium. The host sediment was composed of bioturbated and mottled, orange and tan, silty, very fine sand to very fine sandy, silt. Below the base of the cutbank, probing suggested the presence of 0.6 m of silty fine sand underlain by 0.45 m of very fine sandy, silt followed by 0.05 m of gravel. There were three tabular dikes composed of very fine sandy, silt to silty, very fine sand that were about 6 cm wide near the base of the cutbank and narrowed upsection until they terminated at 36, 38, and 40 cm awl. There was little difference in grain size between the host sediment and dikes, and the dike margins were bioturbated, making the difficult to trace higher in the section. The structural characteristics of the features and their proximity to more obvious dikes at sites MR2 and MR3, described below, support the interpretation that the deformation structures at MR1 are earthquake-induced liquefaction features.

Site MR2 is located 2.3 km downstream from Rt. 654 bridge and along the south bank in a 2 m-high cutbank in Holocene alluvium. Exposure was good in the lower 1.5 m, but poor in the upper 0.5 m. The host sediment was composed of bioturbated, mottled and iron-stained, orange and gray, very fine sandy, silt. Below the base of the cutbank, probing suggested 1.4 m of interbedded silt and sand underlain by 0.1 m of medium to coarse sand. Two sand dikes composed of gray, silty, very fine sand, 2 cm and 3 cm wide, branched and pinched upward and terminated 0.9 m and 1 m awl, respectively (Figure 7). The upper 10 cm of the sand dikes was iron-stained throughout and the subjacent 30 cm of the dikes was mottled. Also, the upper portions of the dikes appeared bioturbated. The larger of the two sand dikes had a strike and dip of N56°W, 83°SW and exhibited flow laminations possibly related to the injection of liquefied sediment. The smaller dike had a strike and dip of N2°E, 88°SW.

Site MR3 is located 9.5 km downstream from Rt. 654 bridge and along the north bank of the river. Similar to MR2, MR3 was in a 2 m-high cutbank in Holocene alluvium. The lower 1.5 m of the cutbank exposed 30 cm of brown silt underlain by 1.1 m of bioturbated and mottled, brown and gray, very fine sandy, silt. As determined with a probe, silt continued for another 0.7 m below the cutbank and was underlain by very fine sandy, silt to a depth of 1.5 m. Two sand dikes, both up to 5 cm wide and composed of silty, very fine sand, extended upsection through mottled, very fine sandy, silt and pinched out at 10 cm and 45 cm above the water level (Figure 8). The dikes were wider and more obvious below the water level and became more disturbed by bioturbation higher in the section. The more prominent dike, with a strike and dip of N64°E, 79°SW, may have extended higher in the section into the brown, silt; however, bioturbation and mottling made it difficult to trace the dike above 45 cm awl.

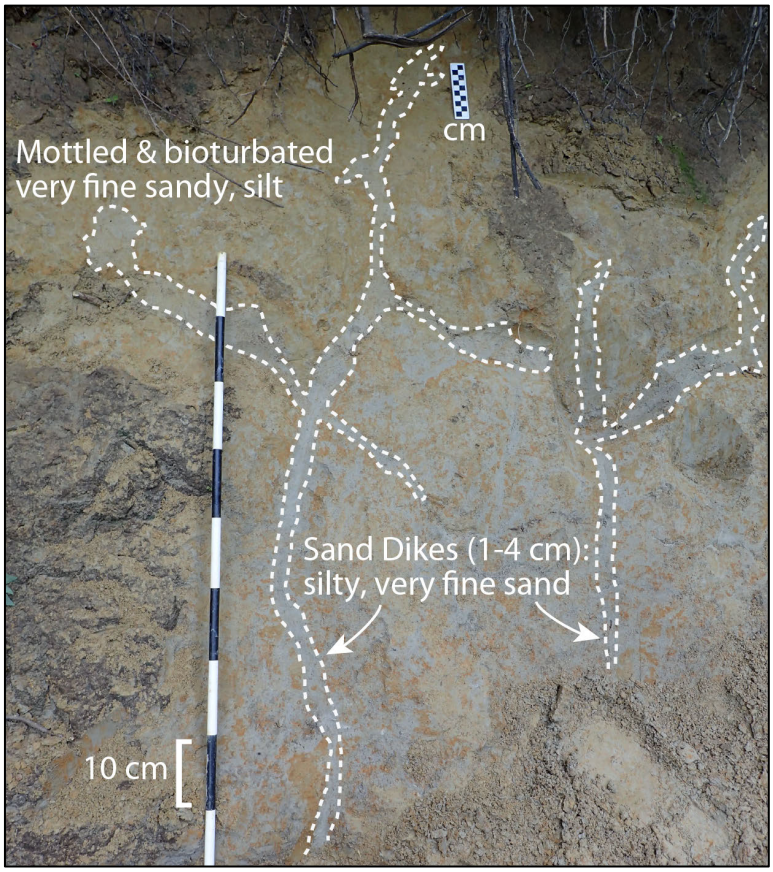

Figure 7. Photograph of sand dikes at site MR2: sand dikes of gray silty, very fine sand extend and branch upsection, crosscutting mottled silt; on small scale, black and white intervals represent centimeters; on large scale, black and white intervals represent decimeters.

Interpretation

The sand dikes site at MR1, MR2, and MR3 along the Mattaponi River are likely to be earthquake-induced liquefaction features. The dikes are composed of silty, very fine sand and occur within host sediment of predominantly very fine sandy, silt. At all three sites, the host sediment is bioturbated and mottled. The sand dikes are more obvious deeper in the section and become more difficult to trace higher in the section where they too are disturbed by bioturbation. The degree of bioturbation and weathering of the host sediment and the sand dikes suggest that they are Holocene in age. Unfortunately, we have no radiocarbon or OSL dates to help estimate the ages of the host sediment and the dikes. We hope to rectify this in the future.

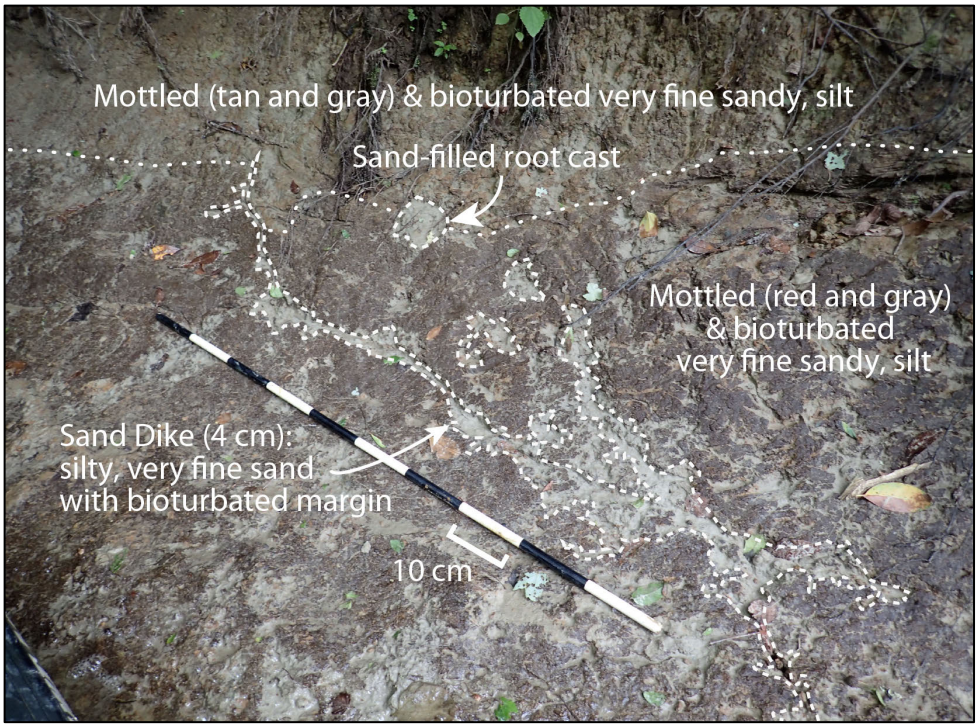

Figure 8. Photograph of sand dike at site MR3: dike of gray silty, very fine sand extends upsection, crosscutting mottled, very fine sandy, silt; the dikes are wider and more obvious below the water level and become more disturbed by bioturbation higher in the section; black and white intervals on scale represent decimeters.

North Anna River

Setting

South of Ruther Glen, we searched an 18 km-long segment of the North Anna River between the Rt. 1 bridge and the confluence of the North and South Anna Rivers, where the two rivers combine to form the Pamunkey (Figure 3). The geology mapped along this segment of the North Anna River is quite complex and includes many units representing time periods from the Holocene to the Upper Paleozoic. We focused our search in Holocene and Pleistocene fluvial deposits often inset into upper and lower Tertiary units of fine to coarse sand and clayey silt or red Triassic siltstone and sandstone. Occasionally, exposures revealed units of Cretaceous orange to yellow, fine to medium sand overlying Triassic units. In other places, the Cretaceous units unconformably overlie the Petersburg granite of Paleozoic age (Weems, R.E., 1986).

Cutbanks ranged from 2-9 m in height and generally provided good exposure of Holocene and Pleistocene sediment. Holocene sediment consisted of interbedded silt and sand with moderate iron-staining and occasional organic layers. Pleistocene sediment occurred beneath Holocene sediment and was composed of bioturbated and mottled, reddish, silt and sand underlain by pebbles and cobbles. These deposits were often inset into Tertiary and Triassic units composed of materials not susceptible to liquefaction. Sediment conducive to the formation of earthquake-induced liquefaction became more prevalent downstream from a cutoff channel about 6 km from the Rt. 1 bridge. From the cutoff channel to the confluence with the South Anna River, cutbanks revealed interbedded silt and sand with thin laminations of organics. Probing below the base of

the cutbank, we found that interbedded silt and sand extends to a depth of at least 1.5 m and often coarsens downward to gravel. The fluvial sediment exposed along the lower 12 km of the North Anna River are likely to be Holocene in age.

Three sites, NR1, NR2, and NR3, were documented along the North Anna River (Figure 3). Two of the three sites contained soft sediment deformation features (NR1 and NR2) and one site was sampled for radiocarbon dating (NR2). The three sites are described below.

Observations

At site NR1, located about 2 km downstream from the Rt. 1 bridge, the cutbank was 2.5-3 m high with upper 2 m was mostly covered by vegetation. The lower 0.5 m of the cutbank revealed interbedded silt and fine sand (4 cm thick), good conditions for the formation of earthquake-induced liquefaction features. Probing below the base of the cutbank suggested interbedded silt and sand to a depth of 1.2 m followed by at least 10 cm of pebbly sand. About 10 cm above the water level, the contact between silt above and sand below was cuspate, with small (7-10 mm) concave downward cusps along the base of the silt layer. The cuspate contact is suggestive of basal erosion related to liquefaction of the underlying sand layer. However, there was no other indication of liquefaction such as foundered clasts, sand dikes, sand diapirs, or load casts along the contact. Therefore, the basal contact might reflect draping of silt over bed forms of the top of the sand layer.

At site NR2, located about 6 km downstream from the Rt. 1 bridge, the cutbank was 3 m high and provided excellent exposure of the lower 1.5 m, where organic-rich silt unconformably overlies interbedded silt and fine sand with crossbedding. At the upstream end of the exposure, the organic-rich silt appears to fill an abandoned channel. Similar to NR1, the contact between silt above and sand below was cuspate, suggesting basal erosion due to liquefaction. However, there was no more definitive indication of earthquake-induced liquefaction. The sedimentary conditions are conducive to the formation of earthquake-induce liquefaction features; but no unequivocal liquefaction features were found at the site.

Site NR3 is located 0.5 km downstream from NR2. At the site, a 4 m-high cutbank provided excellent exposure of the lower 1-1.5 m. The upper 2-2.5 m was covered with vegetation. Interbedded silt and sand with a few, thin organic layers was exposed in the lower part of the cutbank. Probing below the cutbank, the deposit of interbedded silt and sand extended to a depth of at least 1.5 m. No soft-sediment deformation structures were observed in the sediment at this site. However, a piece of wood (NA3-W1) was collected from an organic layer 20 cm above water level and yielded a 2-sigma calibrated radiocarbon age of 295-255, 225-135, 115-110, 95-85, 30- Post 0 (or A.D. 1655-1695, A.D. 1725-1815, A.D. 1835-1840, A.D. 1855-1865, and A.D. 1920-Post 1950), providing age estimate for the sediment along this segment of the river.

Interpretation

At NR1 and NR2, cuspate contacts between silt and sand are suggestive of basal erosion related to earthquake-induced liquefaction. However, no more definitive liquefaction features such as foundered clasts, sand dikes, sand diapirs, or load casts were found at these sites or at NR3. Perhaps the cuspate contacts are indicative of a brief period of liquefaction, not long enough for more definitive features to form. Evenso, these features are equivocal. Dating at NR3 suggests that sediment at the site was deposited since A.D. 1655. Sediment of the 3-4 m-high terrace at

NR1 and NR2 and other sites along the upper part of the river is probably similar in age and provides only a short record relevant to paleoseismic studies.

Pamunkey River

Setting

We searched 21.5 km of the Pamunkey River along two segments. The first segment is between the Rt. 2 bridge north of Hanover and a private boat ramp about 11.5 km downstream on the property of the Hanover Juvenile Correctional Facility. The second segment is a 10 km stretch between the confluence of the North and South Anna Rivers and the Rt. 2 bridge. Geology mapped along the searched portion of the Pamunkey River is similar to that along the North Anna River; however, the Holocene floodplain is much wider here, and therefore, is more likely to include older sediment. Flanking the Holocene floodplain, a Pleistocene terrace composed of sand, pebble, and cobble is underlain by upper and lower Tertiary units, including the upper and lower Chesapeake Group and the Aquia formation. The upper Chesapeake contains fine to medium sand with abundant heavy minerals and iron-cemented sandstone that is generally yellow but sometimes gray where freshly exposed. The lower Chesapeake is composed of gray, clay to sandy clay that weathers to light gray and contains numerous lenses of snail impressions. The lower Chesapeake is underlain by the Aquia formation, a glauconitic, quartz sand containing shells and diatoms. Beneath the Tertiary units is the Cretaceous Patuxent formation composed of firmly packed, white to yellow-orange, fine to medium sand (Weems, R.E., 1986).

Along the 11.5 km segment between the Rt. 2 bridge and the correctional facility, most cutbanks ranged from 1-4.5 m in height and provided good exposure of the lower 2 m. In general, most cutbanks exposed mottled (red and gray) interbedded silt and sand. However, a few exposures revealed mottled, brown and gray, clayey silt and silty clay. Probing below the cutbanks, we found that interbedded silt and sand often extended to at least 1.5 m depth. At a few locations, the probe met refusal at less than 1.5 m depth, possibly in firmly packed Tertiary or Cretaceous units. These older units and overlying Pleistocene deposits of a higher terrace level (~8-10 m high) were often exposed on the outside bends of large meanders. In general, the mottled and iron-stained interbedded silt and sand of the lower terrace level (1-4.5 m high) are likely to be Holocene in age and appeared to be conducive to the formation of liquefaction features.

Along the 10 km segment between the confluence of the North and South Anna Rivers and the Rt. 2 bridge, cutbanks ranged from 2-4.5 m in height and provided good exposure of the lower 1.5-2 m. Sedimentary conditions are similar to the segment downstream from the Rt. 2 bridge. Most exposures revealed mottled, red and gray, interbedded silt and sand with occasional finer-grained deposits of mottled, brown and gray, clayey silt and silty clay. Again, the exposures along the outer bends of large meanders are in a higher terrace composed of Pleistocene deposits underlain by Tertiary and Cretaceous units. The deposits beneath the 2-4.5 m terrace are likely to be Holocene in age and appear to be susceptible to earthquake-induced liquefaction.

Seven sites were documented along the Pamunkey River. Sites PR1, PR2, PR3, PR4, and PR5 are located along the 11.5 km segment downstream from the Rt. 2 bridge. Sites PR6 and PR7 are located between the confluence of the North and South Anna Rivers and the Rt. 2 bridge. Soft-sediment deformation structures likely to be earthquake-induced liquefaction features were found at PR2, PR6, and PR7. At PR4, an apparent fault in Tertiary units was found in a cutbank

exposure of older deposits. Radiocarbon dating of organic samples collected at PR5 and PR6 provide age control for the sediment and soft-sediment deformation structures along the Pamunkey River. The sites and deformation structures are described below.

Observations

Site PR1 is located 1.5 km downstream from the Rt. 2 bridge where there was a 1.5-2 m cutbank on the north side of the river. The lower 1.0 m provided good exposure of mottled, brown and gray, silt underlain by silty sand followed by sand. Probing below the bank suggested that silt extended to a depth of 0.7 m and was underlain by 0.6 m of silty sand followed by 0.2 m of medium to fine sand.

Site PR2 is located about 0.5 km downstream from PR1 where there was a 4-4.5 m cutbank on the south bank. The upper part of the cutbank was heavily vegetated, but the lower 1-1.5 m revealed very mottled, red and gray, silt underlain by somewhat mottled, reddish, very fine sandy, silt (Figure 9). Extensive biotubation, iron-staining, and mottling suggest that sediment at this site is at least several thousands of years old. Probing suggested silt grading to silty sand extended to 1.5 m below the base of the cutbank. Five sand dikes composed of very fine silty sand, possibly originating in the silty sand encountered by the probe, were found crosscutting the mottled, reddish, very fine sandy, silt along a 4.5 m-long section of the cutbank. The dikes ranged in width from 2.7-7.3 cm and extended at least 88 cm above the base of the cutbank. Low in the section, the dikes were tabular structures. Several of the dikes branch and narrow upsection and appeared to have intruded root casts. The upper portions of the dikes were bioturbated and iron-stained along their margins suggesting that they are prehistoric in age.

Across the river from PR1, site PR3 is located along a 2 m-high cutbank, exposing interbedded sand and organic layers that dip downstream. Probing below the base of the cutbank, the same sediment extended to 1.2 m and was underlain by coarser sand to a depth of 1.5 m. Dating of plant material collected from an organic layer 3 cm above the water level yielded a 2-sigma calibrated age of Post 0 (or Post 1950). The sediment at this site is modern and maybe related to the recent formation of a cutoff channel about 0.5 km upstream.

Site PR4 is located 3.6 km downstream from the Rt. 2 bridge in a cutbank exposing faulted Tertiary units of the Chesapeake Group. The apparent normal fault strikes N5°E and dips 55° NW and offsets a contact between a sandy and a clayey unit by 25 cm, down towards the west. The clayey unit is thicker across the fault suggesting an oblique component of movement. No displacement was observed of the contact with an overlying deposit of Pleistocene pebbles and cobbles.

Site PR5 is located 6 km downstream from the Rt. 2 bridge. In this area, the river flows towards the south and the site occurs along the east bank, where sediment wss exposed in a large slump scarp 3.5-4 m high. The exposed sediment included 1.3 m of iron-stained silty fine sand underlain by 1.7 m of white sand followed by 1.5 m of mottled, brown and gray, clayey silt. Probing below the cutbank, we found that clayey silt continued for another 0.5 m and was underlain by at least 1 m of sand. No liquefaction feature was found at this site. However, a sample of charred material was collected from the clayey silt 25 cm above the water level and yielded a 2-sigma calibrated age of 5595-5575, 5550-5475 (or B.C. 3645 - 3625 and B.C. 3600 to 3525). This age may reflect that of the mottled silt along the lower 11.5 km of the river. If so

it provides a maximum constraining age for the sand dikes at site PR2. Dating at or closer to the site would be preferable.

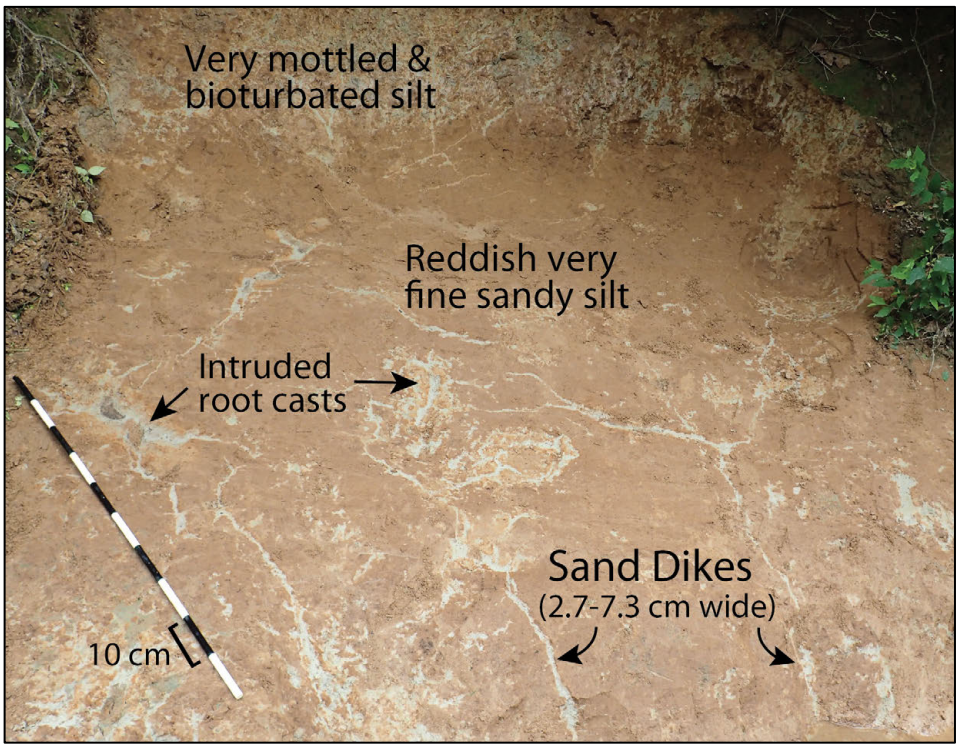

Figure 9. Photographs of sand dikes at site PR2: dikes of gray silty, very fine sand extend up-section, crosscutting mottled, reddish, very fine sandy, silt; the dikes branch and narrow upsection and appear to have intruded root casts; black and white intervals on scale represent decimeters.

Site PR6 is located 2.6 km downriver from the confluence of the North and South Anna Rivers. The site occurs along the west bank of the river where a 2.5-3 m high cutbank exposed interbedded gray silt and medium to fine sand with several organic layers. This deposit appeared to be related to a small creek that enters the Pamunkey about 20 m upstream from the site and to be inset into Pamunkey River deposits. Soft-sediment deformation structures including load casts and pseudonodules occurred in the interbedded silt and sand (Figure 10). These types of structures can form during ordinary depositional processes; however, they can also form as the result of earthquake-induced liquefaction (Sims, 1973 and 2012; Tuttle and Atkinson, 2010). The deformation structures at this site are very similar to those at JR2 that are thought to have formed fairly recently. A sample (PR6-W1) collected from an organic layer at water level yielded a calibrated age of 430-375, 320-285, and 165-155 (or A.D. 1520-1575, A.D. 1630-1665, and A.D. 1785-1795). This result indicates the sediment was deposited and the soft-sediment deformation structures formed since 430 yr B.P. (or A.D. 1520).

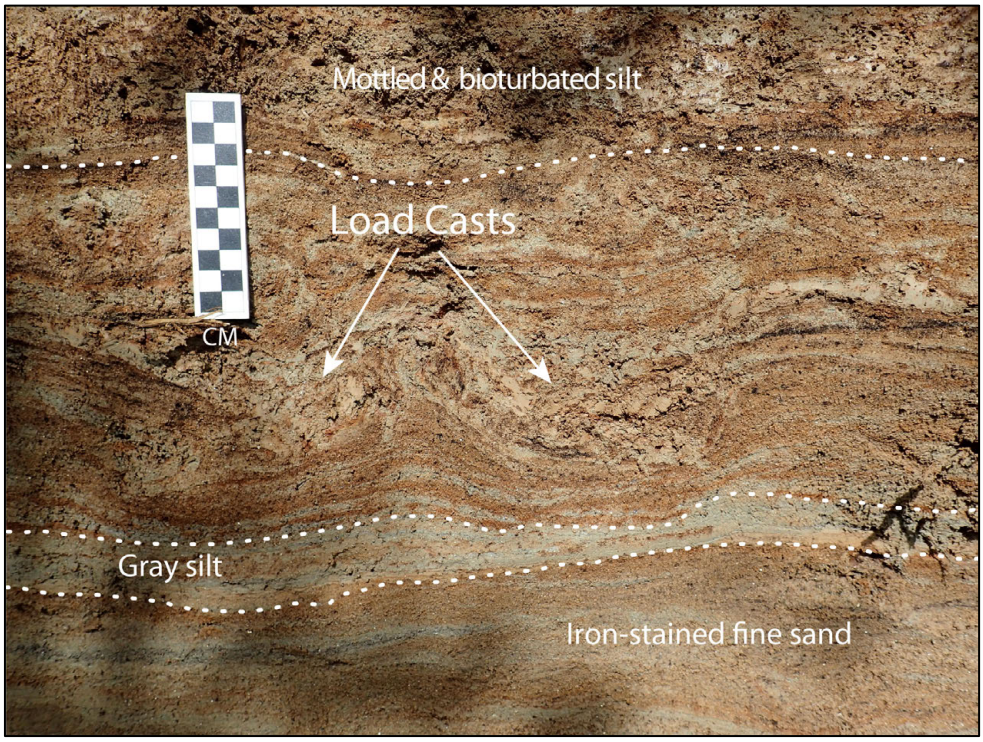

Figure 10. Photograph of soft-sediment deformation structures at site PR6: Load cast and pseudo-nodules (not shown) occur within interbedded sand and silt at the site. C14 dating of plant material from an organic layer at the base of the cutbank suggests that the overlying sediment was deposited and the soft-sediment deformation structures formed since A.D. 1520. Black and white intervals on scale represent centimeters.

Site PR7 is located 7.7 km downstream from the confluence of the North and South Anna Rivers and 2.3 km upstream from the Rt. 2 bridge. The site is on the south bank of the river where there was a 3 m-high cutbank. The upper part of the cutbank was mostly vegetated, but the lower 1-1.5 m was well exposed. About 2.5 m of reddish silt was underlain by 0.5 m of mottled very fine sandy, silt. Probing below the cutbank suggested that sandy silt continued to 0.9 m and was underlain by silty sand to a depth of 1.5 m. Two small (1 cm) sand dikes composed of silty, very fine sand crosscut the mottled, sandy silt and pinch out in the reddish silt at 50 and 70 cm above the water level. The upper portions of both dikes appeared to be bioturbated and the upper 20 cm of the larger dike was iron stained. Although smaller, these dikes are similar to those at PR2 and are likely to be prehistoric in age.

Interpretation

Sand dikes at PR2 and PR7 are interpreted as earthquake-induced liquefaction features. At both sites, the dikes are composed of silty, very fine sand and intrude mottled, red and gray, very fine sandy, silt and silt. The upper portions of the dikes are bioturbated and iron stained suggesting that they are prehistoric in age. Dating of mottled silt at PR5 may provide maximum constraining age for the sand dikes at PR2 and PR7. If so, the dikes formed in the past 5,600 years or since B.C. 3645.

Soft-sediment deformation structures at PR6 are very similar to those at JR2 thought to have formed as the result of liquefaction induced by an earthquake in the recent past. Dating at PR6 suggests that the structures at PR6 formed since 430 yr B.P. (or A.D. 1520) and therefore could be related to the same recent event. Discharge of the Pamunkey River was so low on August 23, 2011 (http://waterdata.usgs.gov/nwis/dvstat?referred_module=sw) that the source beds at PR6 would not have been saturated and therefore could not have liquefied during the 2011 Virginia, earthquake.

Rivanna River and Stigger Creek

Setting

We searched a 10.8 km segment of the Rivanna River from the Rt. 520 bridge near Lake Monticello to the Route 15 bridge at Palmyra (Figure 3). This segment of the Rivanna River is flanked by narrow fluvial terraces. In several places, Precambrian bedrock outcrops along the river banks and in its bed (Virginia Division of Mineral Resources, Geologic Map of Virginia, 1993). Cutbanks in the fluvial terraces ranged from 2 to 6 m in height. The upper part of the cutbanks was mostly covered by grass, shrubs, and tree roots, but exposure of the lower part of the cutbanks was afforded by bank failures, slump scarps, and erosion due to wave action.). Additionally, we searched 0.3 km of lower Stigger Creek, a small tributary entering the Rivanna River 1.3 km downstream from the Rt. 520 bridge, where sand dikes previously had been found (Dominion, 2004). Reconnaissance along the Rivanna River was conducted by canoe; whereas reconnaissance along Stigger Creek was conducted on foot.

At the time of reconnaissance, the Rivanna River was fairly low. The straight 3 km-long portion of the river immediately downriver from the Rt. 520 bridge provided better exposures of sediment than the following 4 km-long segment including two sharp bends. A large bank failure in a 5-6 m-high cutbank just downriver from the bridge revealed mottled silt overlying interbedded silt and sand followed by pebbly sand at water level. In general, this section typifies the stratigraphy of the fluvial deposits composing the narrow terraces along this river segment. Beyond Stigger Creek and before the sharp river bends, a 3 m-high cutbank revealed mottled, brown and gray, silt with a few thin layers of sand. Probing suggested interbedded silt and sand to a depth of 0.85 m where gravel was encountered. Along the upper 3 km of the river, sedimentary conditions appeared to be conducive to the formation of earthquake-induced liquefaction features.

Along the 4 km-long segment including two sharp bends, bedrock outcrops were prevalent and fluvial terraces very narrow and intermittent. There were only a few cutbank exposures in the fluvial terraces. The cutbanks were 2-4.5 m high and exposed about 1 m of reddish silt overlying iron-stained and cemented sand followed by gravel or bedrock. Conditions for the formation of earthquake-induced liquefaction features were not ideal along this segment of the river.

We also searched cutbanks in fluvial deposits along 0.3 km of Stigger Creek. Because of the dry conditions, we were able to traverse the channel bed on foot and examine several good exposures in 2.5-3 m-high cutbanks. The cutbanks revealed reddish silt underlain by mottled, red and gray, silt coarsening downward to silt and sand followed by pebbly sand just at about water level.

One site, RR1, was documented along the Rivanna River and a second site, SC1, was documented at Stigger Creek where sand dikes occur. SC1 occurs in the vicinity of two liquefaction sites found during a previous study and may be one of those sites (Obermeier and McNulty, 1998; Dominion, 2004). Sites RR1 and SC1 are described below.

Observations

About 0.95 km downstream from the Rt. 520 bridge, site RR1 is located on the west side of the Rivanna River. At the site, a 2.5 m-high cutbank was mostly covered with vegetation except for the lower 1 m which very well exposed. The sediment consisted of interbedded silt and thin layers of sand. Probing below the cutbank, sand interbedded with thin layers of ferricrete extended to a depth of 0.6 m. Below 0.6 m ferricrete likely had developed in gravel making it impenetrable with the probe. Plant material was collected from an organic layer 22 cm above the water level within interbedded silt and sand. The sample (RR1-W1) provided a 2-sigma calibrated age of 305-270, 215-145, 20-Post 0 (or A.D. 1645-1680, 1735-1805, 1930-Post 1950). Radiocarbon dating suggests that the interbedded silt and sand deposit and overlying silt of the narrow fluvial terraces at this and other locations along the Rivanna River were deposited during the past 350 years (or since A.D. 1645).

Site SC1 is located along the north side of Stigger Creek about 100 m upstream from its confluence with the Rivanna River. At the site, the upper 1.5 m of a 3 m-high cutbank was partially covered by roots growing in soil developed in reddish silt. The underlying 1.5 m of sediment was well-exposed and consisted of mottled, red and gray, silt with lenses of cobbles and pebbles, underlain by gray, silty fine sand coarsening downward to a silty, medium to fine sand, followed by cobbly and pebbly sand. We found three sand dikes of silty, fine sand, ranging in width from 2-2.7 cm (Figure 11). The dikes originated in the layer of gray, silty, fine sand and terminated in the mottled silt 1.2-1.5 cm above the water level. The upper portion of one of the dikes appeared weathered and to have been disturbed by roots. The upper part of another dike was also weathered and bioturbated and had a 4-cm wide bulbous termination. The two larger dikes had northwest strikes and dipped steeply to the northeast. A sediment sample (SC1-1) was collected from the source layer of the dikes and yielded an OSL age of 9020 ± 550 (or date of B.C. 6460-7560). OSL dating suggests that the source layer of the dikes was deposited about 9 ka (thousand years ago) and the dikes formed since B.C. 7560. Dating of the source bed provides a maximum age, but not necessarily a close maximum age, for the dikes. Weathering and bioturbation of the upper portion of the dikes suggest that they are prehistoric in age.

Interpretations

Much of the sediment composing the narrow fluvial terraces along the 10.8 km segment of the Rivanna River was deposited since A.D. 1645 and therefore would not contain a liquefaction record of paleoearthquakes. Sediment exposed along Stigger Creek, and possibly other tributaries to the Rivanna River, is considerably older, dating back to B.C. 7560. As seen at site SC1, sand dikes interpreted to be earthquake-induced liquefaction features occur in this older sediment. The dikes originate in a silty, fine sand layer and intrude overlying mottled, red and gray, silt. The upper portions of the dikes are weathered and bioturbated suggesting that they are prehistoric in age. OSL dating of the source layer of the dikes at SC1 suggest that they formed since B.C. 7560.

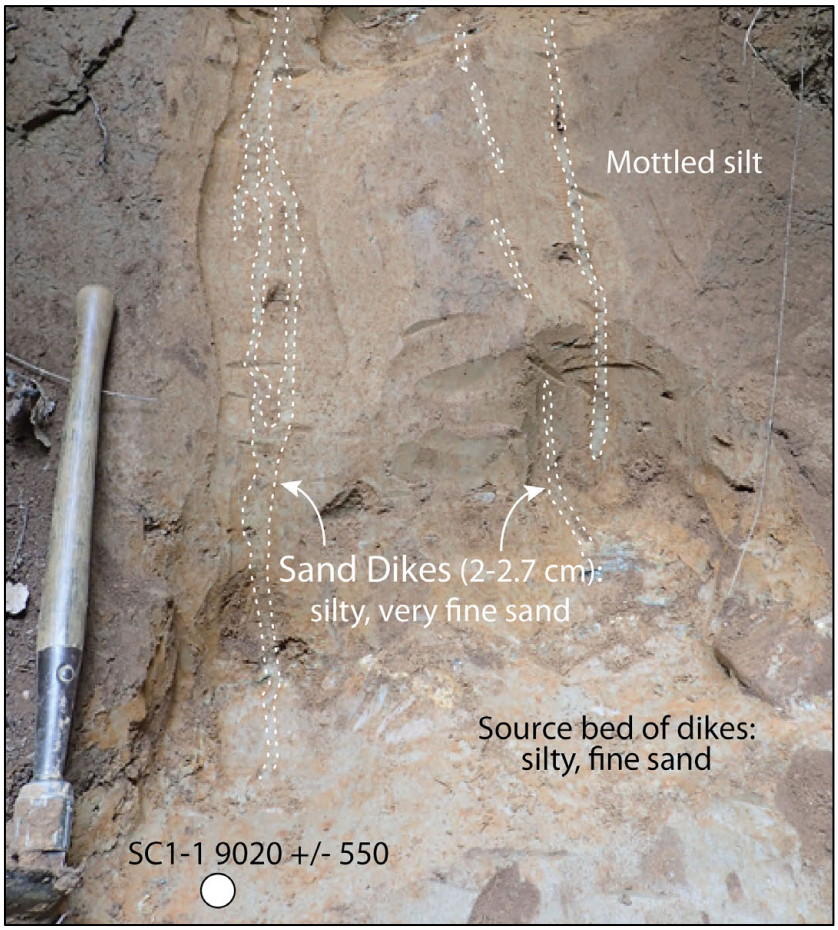

Figure 11. Photograph of sand dikes at site SC1: Sand dikes originate in layer of gray, silty, fine sand and extend upsection, crosscutting mottled silt. White circle indicates approximate location of OSL sample. The OSL age is relative to A.D. 2010. For scale, shovel handle is 50 centimeters in length.

South Anna River

Setting

South of Mineral and between the Rt. 605 and Rt. 699 bridges, we resurveyed a 10 km segment of the South Anna River, where possible paleoliquefaction features were found during a post-earthquake survey in November 2011 (Tuttle and Busch, 2011) (Figure 3). The purpose of the new survey was to reexamine possible paleoliquefaction features at several sites when the river level was lower and more of the sedimentary section exposed, to look for additional liquefaction features, and to collect samples for dating. The geology mapped along this portion of the South Anna River is quite complex representing time periods from the Paleozoic to the Holocene. Bedrock of volcanic rocks of the Chopawamsic Formation that have been metamorphosed to amphibolite facies (Spears, 2013) outcrops along the upper 4 km and the lower 1.2 km of the river segment. We focused our search in Holocene fluvial sediment that forms floodplains along the river.

Cutbanks ranged from 2-3 m in height. The upper 0.5-1 m of the cutbank was mostly covered by vegetation, but the lower section was very well exposed. Recent silt that had covered the lower 0.5 m of the banks in 2011 had been washed away. In general, sediment consisted of mottled, red and gray, silt underlain by mottled, red and gray, very fine sandy, silt or silty, very fine sand followed by interbedded silt and sand. Probing below the cutbanks, we found that very fine sandy, silt or silty, very fine sand or interbedded silt and sand extended to a depth of 0.7-1.5 m and often coarsened downward to a pebbly sand in which ferricrete had formed.

Three sites, SoAR5, SoAR7, and SoAR8 that had been found in 2011 were revisited and one new site, SoAR100, was documented along the South Anna River (Figure 3). Sand dikes occur at the four sites. Radiocarbon dating of an organic sample at SoAR100 and OSL dating of a sediment sample at SoAR7 provide age estimates of the host sediment and maximum constraining ages for the sand dikes. The five sites are described below.

Observations

Site SoAR5, is located about 3.75 km downstream from the Rt. 605 bridge, along the north side of the river, where only the lower 1 m of the bank was exposed. The bank was composed of mottled, red and yellow, silt. Probing beneath the bank, we found that silt continued for 50 cm and was underlain by silty, very fine sand that coarsened to pebbly sand at 70 cm. Several dikes, 1-3.5 cm wide, of silty, very fine sand appeared to have intruded pre-existing cracks and root casts. The dikes were very weathered suggesting that they are prehistoric in age.

Site SoAR7, is located about 4.5 km downstream from the Rt. 605 bridge, where there was a 2 m-high cutbank along the west side of the river. The upper 1 m was composed of mottled, brown and tan, interbedded silt and sand and the lower 1 m was composed of mottled, red and gray, silt. Probing below the cutbank, silt continued for 10 cm, was underlain by 90 cm of silty, very fine sand, and was followed by silt to a depth of 150 cm. Several dikes, 1-1.5 cm wide, of silty, very fine sand crosscut the mottled silt and, like the dikes at SoAR5, appeared to have intruded pre-existing cracks and root casts. A sediment sample (SOAR7-1) was collected from the mottled silt crosscut by the dikes and yielded an OSL age of 8720 ± 500 yr (or date of B.C. 7210-6210) (Table 2). OSL dating of the host sediment provides a maximum constraining age, but not necessarily a close maximum age, for the dikes and suggests they formed after B.C. 7210.

Site SoAR8, is located about 9 km downstream from the Rt. 605 bridge, where there was a 2.5 m-high cutbank along the east side of the river. The upper 0.5-1 m of the cutbank was covered by vegetation, but the lower 1.5 m was well exposed and composed of bioturbated and mottled, red and gray, silt and silty, very fine sand. Probing below the cutbank, interbedded silt and silty, very fine sand continued for 1.1 m and was underlain by 10 cm of pebbly sand. At 1.2 m depth, we could not push the probe any deeper probably due to ferricrete. A sand dike, 1-3 cm wide, of silty, very fine sand crosscut the mottled silty, very fine sand, branched laterally to form a sill and upward to form several smaller dikes (Figure 12). One of these smaller dikes extended upsection and appeared to have intruded root casts. The upper 60 cm of the dike was especially weathered and mottling occurred for another 60 cm below that.

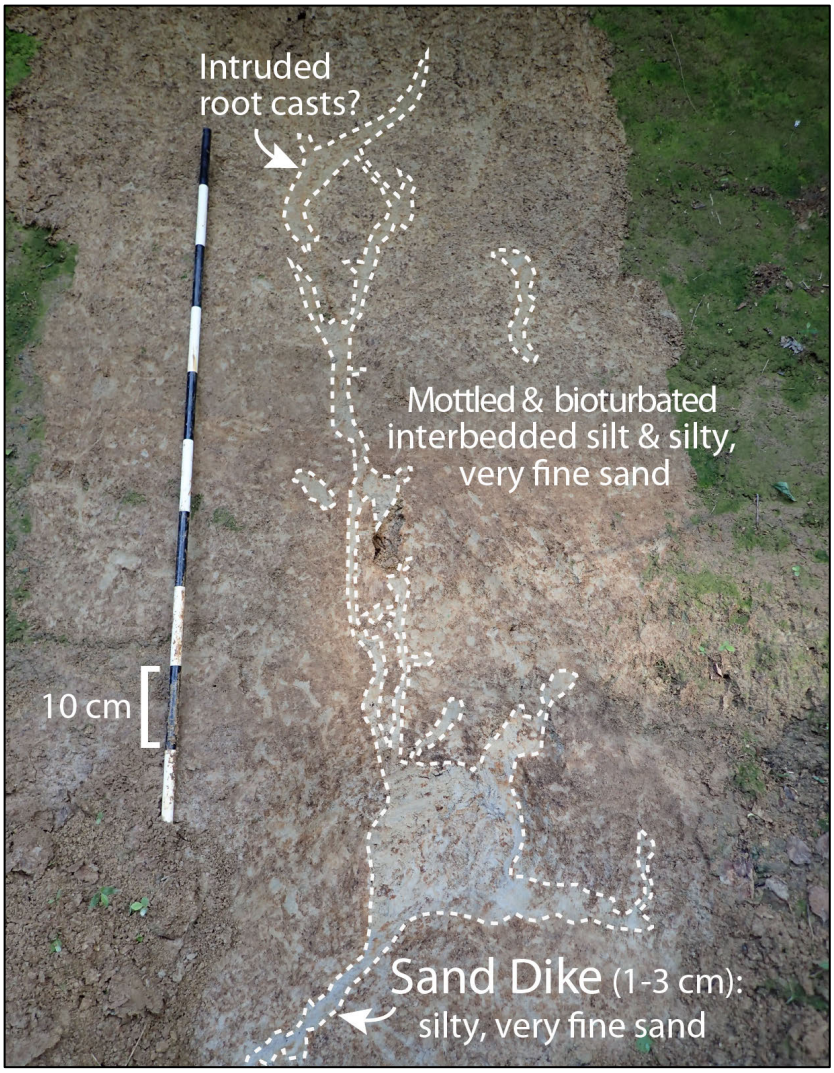

Figure 12. Photograph of sand dike at site SoAR8*: dike of gray, silty, very fine sand extends upsection, crosscutting mottled and bioturbated silt and silty, very fine sand; lower in the section the dike is tabular and has distinct margins; higher in the section it branches laterally to form a sill and smaller dikes. The dikes that extended higher in the section appeared to have intruded root casts. Black and white intervals on scale represent decimeters.*

Site SoAR100, is located about 2.5 km downstream from the Rt. 605 bridge, where a 2-3 m-high cutbank occurred along the north bank of the river. The upper portion of the cutbank was covered by poison ivy, but the lower 1-1.25 m was well exposed and composed of bioturbated and mottled, red and gray, silt. Augering below the cutbank, we found interbedded silt and sand extended to 1.15 m depth and was underlain by silty, very fine sand that coarsened downward to pebbly sand that became impenetrable at 1.35 m depth. A discontinuous dike of silty, very fine sand extended upsection through the mottled silt and terminated about 65 cm above the water level (Figure 13). The upper portion of the dike was bioturbated and appeared to have intruded a pre-existing root cast. Plant material was recovered from the silty sand layer, possibly the source bed of the dike, at 1.25 m below the base of the cutbank. The sample, SoAR100-C1, yielded a 2-sigma calibrated age of 4435-4290 yr B.P. (or B.C. 2485-2340). C14 dating suggests that the

sand dikes formed since 4435 yr B.P (or B.C. 2485). The degree of bioturbation of the dike suggests that it is prehistoric in age.

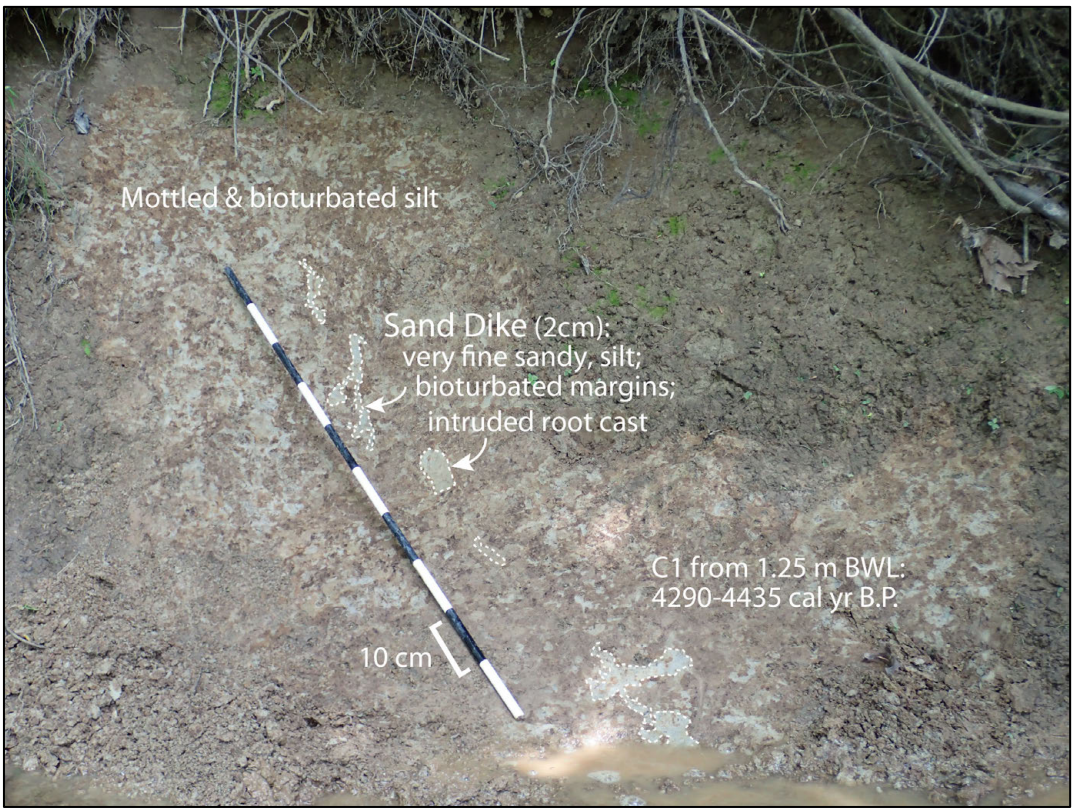

Figure 13. Photograph of sand dike at site SoAR100*: dike of gray silty, very fine sand extends upsection, crosscutting mottled and bioturbated, silt; the dike is more obvious at and below water level and becomes discontinuous and bioturbated higher in the section, making it difficult to trace; C14 result of sample SoAR100-C1 collected from sand layer at depth is shown as range of calibrated radiocarbon ages in years B.P. (or before A.D. 1950). On large scale, black and white intervals represent decimeters.*

Interpretations

Sand dikes and sills at SoAR5, SoAR7, SoAR8, and SoAR100, are thought to be earthquake-induced liquefaction features. The liquefaction features are composed of silty, very fine sand and intrude mottled, red and gray, silt and very fine sandy, silt. The dikes appear to have intruded pre-existing cracks and root casts. The upper portions of the dikes are weathered and bioturbated suggesting that they are prehistoric in age. Sediment at the four sites is probably similar in age. Dating of a sand layer, possibly the source bed of a dike, at SoAR100 and of mottled silt crosscut by dikes at SoAR7 suggest that the sediment was deposited during the Early and Middle Holocene and that the dikes along this segment of the South Anna River formed sometime after 4435 yr B.P. (or B.C. 2485).

CONCLUSIONS

Sand dikes, sills and soft-sediment deformation features, interpreted to be earthquake-induced liquefaction features, were studied at 13 sites within 55 km of the epicenter of the 2011 moment

magnitude, **M**, 5.8 Virginia, earthquake. These features were found during systematic surveys of cutbank exposures along 119 km of six rivers: the South Anna River, where likely paleoliquefaction features were found within 5 km of the epicenter following the 2011 earthquake; the Mattaponi, North Anna, and Pamunkey Rivers east of the Fall Line, where liquefiable sediments are more common than in the epicentral area of the 2011 earthquake; and the James and Rivanna (and tributary Stigger Creek) Rivers, where sand dikes were found during an earlier paleoliquefaction study in the 1990s.

Liquefaction features include sand dikes and sills, composed predominantly of silty, fine sand, and strata-bound soft-sediment deformation features, including load casts and pseudonodules, that formed within interbedded sand and silt. In general, the dikes branch and pinch upward. Degree of bioturbation and weathering of liquefaction features, as well as dating of host sediment, suggest that the liquefaction features formed during at least two different events - a recent event, probably in the past 500 years, and a paleoearthquake sometime in the past 4,500 years. Liquefaction features that may have formed during the relatively recent earthquake include sand dikes up to 3 cm wide at JR1 that formed since 305 calibrated yr B.P. (before A.D. 1950) and strata-bound soft-sediment deformation structures at nearby JR2 and at PR6 that formed since 305 yr B.P. and 430 yr B.P., respectively. Dating at the three sites suggest that the features formed during the past 500 years, and possibly during the past 350 years. Exhibiting a greater degree of bioturbation and weathering, liquefaction features likely to have formed during the earlier earthquake occur at MR1, MR2, MR3, PR2, PR7, SC1, SoAR5, SoAR7, SoAR8, and SoAR100. These sand dikes range up to 7 cm wide with the largest occurring at sites along the Mattaponi and Pamunkey Rivers. Radiocarbon dating of organic samples from host sediment at PR5 and SoAR100 provides maximum constraining ages of 5595-5475 calibrated yr B.P. (before A.D. 1950) and 4435-4290 calibrated yr B.P., respectively, of the paleoliquefaction features. OSL dating of sediment at SC1 and SoAR7 also provides maximum constraining ages of 9020 ± 550 yr (before A.D. 2010) and 8720 ± 500 yr, respectively, of the paleoliquefaction features. Except for the recent deposit at JR1, radiocarbon ages of sediment are younger than OSL ages. In our age estimates of sediment and liquefaction features, we give preference to radiocarbon ages over OSL ages. Until there is evidence to suggest otherwise, we assume that the more weathered liquefaction features formed during a single event during the Late Holocene. The youngest maximum constraining age suggests that the event occurred in the past 4,500 years.

Currently, the recent event is represented by liquefaction features at only three sites. The three sites occur in the southeastern portion of the liquefaction field shown on Figure 3. Perhaps an earthquake in this area or farther to the southeast is responsible for the features. Uncertainties will remain large until additional data can be brought to bear on the interpretation of this event. The paleoliquefaction features attributed to a Late Holocene event are larger than and more broadly distributed than those that formed during the 2011 Virginia, earthquake suggesting that the paleoearthquake was larger than **M** 5.8. In addition, the paleoliquefaction features are larger at the eastern sites suggesting that either the sediment is more susceptible to liquefaction east of the Fall Line or that ground shaking during the Late Holocene paleoearthquake was stronger in the east. If the later, the paleoearthquake may have been located farther east than the 2011 Virginia, earthquake.

To date, Late Holocene liquefaction features, including sand dikes, have been found within a 3,200 km^2 area (radius of ~45 km) in the northeastern quadrant of the CVSZ. According to the

relation of Castilla and Audemard (2007), an earthquake of **M** ≥ 6 would be necessary to induce liquefaction leading to the formation of sand blows over such an area (Figure 14). It should be noted that no sand blows have yet been found in association with the sand dikes. However, given the relatively small size of the features and the high degree of bioturbation, sand blows easily could have been destroyed. Additional study is needed to map the full extent and to constrain the ages of the relatively recent and Late Holocene liquefaction features in order to better estimate timing, source areas, and magnitudes of the paleoearthquakes. Information about these events in the CVSZ will contribute to national and regional assessments of earthquake hazard.

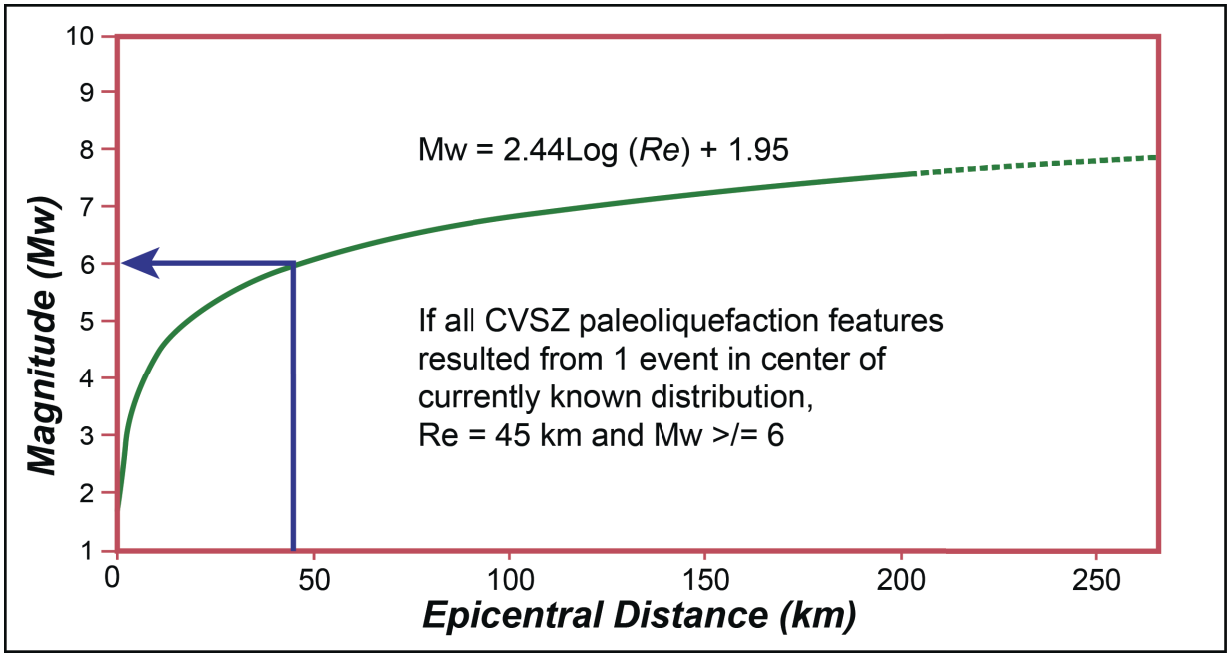

Figure 14. Earthquake magnitude-epicentral distance to liquefaction relation developed from worldwide liquefaction data set (modified from Castilla and Audemard, 2007; drafted by M. Carter).

REFERENCES CITED

Bollinger, G. A., and Sibol, M. S., 1985, Seismicity, seismic reflection studies, gravity and geology of the Central Virginia seismic zone, Part I. Seismicity, Geological Society of America Bulletin, v. 96, p. 49-57.

Carter, M. W., 2015, Characterizing pedogenic and potential paleoseismic features in South Anna River alluvium: epicentral region of the 2011 earthquake Central Virginia seismic zone, Presentation at the 2015 Virginia Geological Research Symposium.

Carter, M. W., Tuttle, M. P., and Dunahue, J., 2016, Characteristics of paleoliquefaction features in the Central Virginia seismic zone, Geological Society of America, Abstracts with Programs, v. 48, n. 3, doi: 10.1130/abs/2016SE-273045.

Castilla, R. A., and Audemard, F. A., 2007, Sand blows as a potential tool for magnitude estimation of pre-instrumental earthquakes, Journal of Seismology, v. 11, p. 473-487.

Chapman, M. C., 2013, On the rupture process of the 23 August 2011 Virginia earthquake: Seismological Society of America Bulletin, v. 103, no. 2A, p. 613–628, doi:10.1785/0120120229.

Cubrinovski, M., Green, R. A., Wotherspoon, L. (editors), Allen, J., Bradley, B., Bradshaw, A., Bray, J., Cubrinovski, M., DePascale, G., Green, R. A., Orense, R., O'Rourke, Pender, M., Rix, G., Wells, D., Wood, C., and Wotherspoon, L. (contributing authors in alphabetical order), 2011, Geotechnical reconnaissance of the 2011 Christchurch, New Zealand earthquake, Geotechnical Extreme Events Reconnaissance Association Report No. GEER-027.

Dominion, 2004, Response to request for additional information no. 3, North Anna Early Site Permit Application, Dominion Nuclear North Anna, LLC, U.S. Nuclear Regulatory Commission, Report ML042800292, 110 p.

Ellsworth, W. L., Imanishi, K., Luetgert, J. H., and Pratt, T. L., 2011, The Mw 5.8 Virginia earthquake of August 23, 2011: A high stress drop event in a critically stressed crust, Abstract, 83rd Annual Meeting of the Eastern Section of the Seismological Society of America, October, 2011, Little Rock, Arkansas, p. 40.

Green, R., Lasley, S., Carter, M. W., Munsey, J. W., Maurer, B. W., Tuttle, M. P., 2015, Geotechnical aspects in the epicentral region of the 2011 Mw 5.8 Mineral, Virginia, earthquake, in Horton, J.W., Jr., Chapman, M.C., and Green, R.A., eds., The 2011 Mineral, Virginia, earthquake, and its significance for seismic hazards in eastern North America: Geological Society of America Special Paper 509, doi:10.1130/2015.2509(09).

Horton, J. W., Jr., McNamara, D. E., Shah, A. K., Gilmer, A. K., Carter, A. M., Burton, W. C., Harrison, R. W., Carter, M. W., Herrmann, R. B., and Snyder, S. L., 2012, Preliminary analysis of magnitude 5.8 Virginia earthquake causative fault and subsidiary faults illuminated by aftershocks: Geological Society of America Abstracts with Programs, v. 44, no. 7, p. 381.

Marr, J. D., Jr., 2002, Geologic map of the western portion of the Richmond 30 X 60 minute quadrangle, Virginia, Virginia Division of Mineral Resources, Publication 165, scale 1:100,000.

Martin, J. R. (editor), Benson, C., Chapman, M., Eddy, M., Green, R., Kammerer, A., Lasley, S., Lazarte, C., Nikolaou, S., Tanyu, B., and Tuttle, M. (contributing authors in alphabetical order), 2011, Geotechnical quick report on the affected region of the 23 August 2011 M5.8 central Virginia earthquake near Mineral, Virginia, Geotechnical Extreme Events Reconnaissance Association Report No. GEER-026.

Obermeier, S. F., and McNulty, W. E., 1998, Paleoliquefaction evidence for seismic quiescence in central Virginia during late and middle Holocene time, EOS, Transactions of the American Geophysical Union, v. 79, no. 17, Spring Meeting Supplement, Abstract T41A-9.

Petersen, M. D., Frankel, A. D., Harmsen, S. C., Mueller, C. S., Haller, K. M., Wheeler, R. L., Wesson, R. L., Zeng, Y., Boyd, O. S., Perkins, D. M., Luco, N., Field, E. H., Wills, C. J., and Rukstales, K. S., 2008, Documentation for the 2008 update of the United States National Seismic Hazard Maps, U.S. Geological Survey Open-File Report 2008-1128, 61 p.

Prescott, J. R., and Hutton, J. T., 1994, Cosmic ray contribution to dose rates for luminescence and ERS dating: large depth and long-term time variations, Radiation measurements v. 23, p. 497-500.

Sims, J. D., 1973, Earthquake-induced structures in sediments of Van Norman Lake, San Fernando California, Science, v. 182, p. 161-163.

Sims, J. D., 2012, Earthquake-induced load casts, pseudonodules, ball-and-pillow, and convolute lamination: Additional deformation structures for paleoseismic studies, *in* Cox, R. T., Tuttle, M. P., Boyd, O. S., and Locat, J., eds.,"Recent Advances in North American Paleoseismology and Neotectonics East of the Rockies," Geological Society of America, Special Paper 493, p. 191-201.

Soller, D. R., and Reheis, M. C., 2004, Surficial materials in the conterminous United States, U.S. Geological Survey, Open-file Report 03-275, scale 1:5,000,000, http://pubs.usgs.gov/of/2003/of03-275/.

Spears, D. B., 2012, Geologic framework of the central Virginia seismic zone, Geological Society of America, Abstracts with Programs, v. 44, no. 5, p. 14.

Spears, D. B., 2013, Geology of the Pendleton quadrangle, Virginia, with notes on the August 2011 Mineral earthquake, Geological Society of America, Abstracts with Programs, v. 45, n. 7, p. 378.

Spears, D. B., Owens, B. E., and Bailey, C. M., 2004, The Goochland-Chopawamsic terrane boundary, central Virginia piedmont, US Geological Survey Circular 1264, p. 223-231.

Talma, A. S. and Vogel, J. C., 1993, A simplified approach to calibrating C14 dates, Radiocarbon, v. 35, p. 317-322.

Tarr, A. C., and Wheeler, R. L., 2006, Earthquakes in Virginia and vicinity 1774 - 2004: U.S. Geological Survey Open-File Report 2006–1017.

Tuttle, M., 2015, Paleoliquefaction studies: learning from historical and modern cases of liquefaction and dating paleoliquefaction features, U.S. NRC Paleoliquefaction training workshop in the New Madrid seismic zone, U.S. NRC ADAMS.

Tuttle, M., Law, T., Seeber, L., and Jacob, K., 1990, Liquefaction and ground failure in Ferland, Quebec, triggered by the 1988 Saguenay Earthquake, Canadian Geotechnical Journal, v. 27, p. 580-589.

Tuttle, M. P., and Atkinson, G. M., 2010, Localization of large earthquakes in the Charlevoix seismic zone, Quebec, Canada during the past 10,000 years, Seismological Research Letters, v. 81, n. 1, p. 18-25.

Tuttle, M. P., and Busch, T. A., 2011, Post-earthquake survey following the 2011 M 5.8 Virginia event, Preliminary report to the U.S. Nuclear Regulatory Commission, 2 p.

Tuttle, M. P., and Hartleb, R., 2012, Central and eastern U.S. paleoliquefaction database, uncertainties associated with paleoliquefaction data, and guidance for seismic source characterization, Appendix E. *in* The Central and Eastern U.S. Seismic Source Characterization for Nuclear Facilities, Technical Report, EPRI, Palo Alto, CA, U.S. DOE, and U.S. NRC, 135 p. plus database.

Tuttle, M., Carter, M. W., Dunahue, J., 2015, Paleoliquefaction study of the earthquake potential of the Central Virginia seismic zone, Geological Society of America, Abstracts with Programs, v. 47, n. 7, p. 466.

Virginia Division of Mineral Resources, 1993, Geologic Map of Virginia, Virginia Department of Mines, Minerals, and Energy, Series 39-4, scale 1:500,000.

Vogel, J. C., Fuls, A., Visser, E., and Becker, B., 1993, Pretoria calibration curve for short-lived samples, Radiocarbon, v. 33, p. 73-86.

Weems, R.E., 1986, Geology of the Ashland quadrangle, Virginia: Virginia Division of Mineral Resources, Publication 64, scale 1:24,000.

Wheeler, R. L., and Johnston, A. C., 1992, Geologic implications of earthquake source parameters in central and eastern North America, Seismological Research Letters, v. 63, no. 4, p. 491-505.

BIBLIOGRAPHY OF RELATED PUBLICATIONS

Carter, M. W., Tuttle, M. P., and Dunahue, J., 2016, Characteristics of paleoliquefaction features in the Central Virginia seismic zone, Geological Society of America, Abstracts with Programs, v. 48, n. 3, doi: 10.1130/abs/2016SE-273045.

Tuttle, M., 2015, Paleoliquefaction studies: learning from historical and modern cases of liquefaction and dating paleoliquefaction features, U.S. NRC Paleoliquefaction training workshop in the New Madrid seismic zone, U.S. NRC ADAMS.

Tuttle, M. P., and Busch, T. A., 2011, Post-earthquake survey following the 2011 M 5.8 Virginia event, Preliminary report to the U.S. Nuclear Regulatory Commission, 2 p.

Tuttle, M. P., and Hartleb, R., 2012, Central and eastern U.S. paleoliquefaction database, uncertainties associated with paleoliquefaction data, and guidance for seismic source characterization, Appendix E. *in* The Central and Eastern U.S. Seismic Source Characterization for Nuclear Facilities, Technical Report, EPRI, Palo Alto, CA, U.S. DOE, and U.S. NRC, 135 p. plus database.

Tuttle, M., Carter, M. W., Dunahue, J., 2015, Paleoliquefaction study of the earthquake potential of the Central Virginia seismic zone, Geological Society of America, Abstracts with Programs, v. 47, n. 7, p. 466.